

Editor-in-Chief

Aschalew Gelaw

Editorial Manager

Tesfahun Melese

Associate Editors

Abrham Wondmu

Amare Teshome

Destaw Fetene

Mengistu Melkamu

Tadesse Guadu

Wubet Birhan

Language Editor

Mary T. White

Managing Editor

Abebech Molla

EDITORIAL

Emergence and spread of Carbapenemase producing Gram negative bacteria in Ethiopia: a call for action

Mizan Kindu.....1

ORIGINAL ARTICLE

Common chest radiographic patterns and associated factors of drug-resistant tuberculosis disease at the University of Gondar Comprehensive Specialized Hospital, Northwest Ethiopia, 2020.

Samuel Addis Mihiretie, Temesgen Tadesse Alemayehu, Tewodros Tsegaye Ayele, Getahun Molla Kassa3

Antioxidant Activity Of The Leaf Extracts of *Boscia coriacea* Graells And *Uvaria leptocladon* Oliv

Sintayehu Tsegaye Tseha, Yalemtehay Mekonnen, Asnake Desalegn, Mesfin Getachew Paulos Getachew,

Melaku Wondafarsh13

Anatomic variation of the palmaris longus muscle: A study using the Anatomage Table

Abebe Muche, Abebe Bekele23

Investigation of Hepatotoxic Effect of Cement-Dust in Occupationally Exposed Individuals in Malet, Kwara State, Nigeria, 2022

Akeem Olayinka Busari, Nimotallahi Temitope Omoteji, Idris Yahaya Mohammed31

INSTRUCTIONS TO AUTHORS

SUBSCRIPTION TO THE ETHIOPIAN JOURNAL OF HEALTH AND BIOMEDICAL SCIENCES



Scholarly Organ of the College of Medicine and Health Sciences, University of Gondar

P. O. Box 196, Gondar, Ethiopia
E-mail: ejhbsemhs@gmail.com
Website: www.uog.edu.et
Tel.: +251-582-11-95-24

Emergence and spread of carbapenemase producing Gram negative bacteria in Ethiopia: a call for action

Mizan Kindu^{1*}

¹University of Gondar, College of Medicine and Health Sciences, School of Biomedical and Laboratory Sciences, Department of Medical Microbiology

Corresponding author: mizankindu00@gmail.com

Citation: Kindu M. Emergence and spread of Carbapenemase producing Gram negative bacteria in Ethiopia: a call for action. Ethiop J Health Biomed Sci 2024;14(2):1-2.

DOI: <https://doi.org/10.20372/ejhbs.v14i2.1007>

Article History

Received: December 18, 2024

Revised: December 23, 2024

Published: December 31, 2024

Keywords: Gram negative, carbapenemase, carbapenem, Ethiopia

Publisher: University of Gondar

Editorial

Carbapenems are considered last-resort antibiotics used for the treatment of multidrug-resistant (MDR) Gram negative bacterial (GNB) infection, particularly in hospital settings. However, the emergence of carbapenem resistant bacteria is threatening the effectiveness of these vital antibiotics (1). Globally, the most common resistance mechanism to carbapenems is the production of carbapenemase enzymes (2).

The worldwide distribution of carbapenemases is dynamic, with emerging resistance hotspots. The spread of carbapenem resistant bacteria is facilitated by factors such as travel, medical tourism, and antibiotic overuse. Globally, the most common carbapenemases include *K. pneumoniae* carbapenemases (KPC), New Delhi metallo-β-lactamases (NDM), Verona integron encoded metallo-β-lactamases (VIM), imipenemase (IMP) and oxacillinases (OXA), such as OXA-23, OXA-58, and OXA-48 (2). The distribution of these enzymes varies globally. NDM is prevalent in South Asia, the Middle East, and is increasingly found in Africa and Europe, while KPC dominates in North and South America, Southern Europe, and China. VIM and IMP are common in Europe, South America, and Asia. OXA-48 is widespread in Turkey, North Africa, and Europe, whereas OXA-23 and OXA-58 are frequently detected across Asia, South America, and Africa (3).

In Ethiopia, the occurrence of carbapenemase-producing GNB was first reported in 2017, with *A. baumannii* producing NDM (4). Since then, additional studies have revealed the presence of a variety of carbapenemases, including NDM, OXA-48, OXA-23, OXA-58, OXA-51-like, and KPC-42. These carbapenemases have been detected in a range of pathogens such as *K. pneumoniae*, *A. baumannii*, *P. aeruginosa*, *E. coli*, and other *Enterobacteriaceae* isolated from both patients and environmental samples (5-10). Among these, NDM is the most prevalent carbapenemase detected in Ethiopian isolates. Moreover, co-harboring of multiple carbapenemases, mostly in combination with NDM, has been fre-

Copyright: © 2024 Kindu et al. This is an open access article distributed under the terms of the Creative Commons Attribution-NonCommercial 4.0 (CC BY NC 4.0) License, which permits unrestricted use, distribution, and reproduction in any medium, provided the original author and source are credited.

quently reported, particularly in *K. pneumoniae* and *A. baumannii*. This co-resistance significantly complicates treatment options, making it more challenging to manage infections (6, 7, 9, 10). The few available studies in Ethiopia reported an alarming rise in carbapenem-resistant pathogens in the country and recommended the urgent need for enhanced surveillance, infection control measures, and antimicrobial stewardship to mitigate the threat of MDR infections. Therefore, further research to better understand the epidemiology of carbapenem-resistant bacteria in Ethiopia, and capacity-building initiatives for healthcare providers are crucial for early detection and effective management of MDR infections.

Reference

1. Mancuso G, De Gaetano S, Midiri A, Zummo S and Biondo C. The Challenge of overcoming antibiotic resistance in carbapenem-resistant Gram-negative bacteria: "Attack on Titan". *Microorganisms*. 2023;11(8):1912.
2. Abou-assy RS, Aly MM, Amasha RH, Jastaniah S, Alammari F and Shamrani M. Carbapenem Resistance Mechanisms, Carbapenemase Genes Dissemination, and Laboratory Detection Methods: A Review. *International Journal of Pharmaceutical Research and Allied Sciences*. 2023;12(1-2023):123-38.
3. Hammoudi Halat D and Ayoub Moubareck C. The current burden of carbapenemases: review of significant properties and dissemination among gram-negative bacteria. *Antibiotics*. 2020;9(4):186.
4. Pritsch M, Zeynudin A, Messerer M, Baumer S, Liegl G, Schubert S, et al. First report on bla NDM-1-producing *Acinetobacter baumannii* in three clinical isolates from Ethiopia. *BMC Infect Dis*. 2017;17:1-7.
5. Kindu M, Moges F, Ashagrie D, Tigabu Z and Gelaw B. Multidrug-resistant and carbapenemase-producing critical gram-negative bacteria isolated from the intensive care unit environment in Amhara region, Ethiopia. *PLoS One*. 2023;18(11):e0295286.
6. Gashaw M, Gudina EK, Ali S, Gabriele L, Seeholzer T, Alemu B, et al. Molecular characterization of carbapenem-resistance in Gram-negative isolates obtained from clinical samples at Jimma Medical Center, Ethiopia. *Frontiers in microbiology*. 2024;15:1336387.
7. Seman A, Mihret A, Sebre S, Awoke T, Yeshitela B, Yitayew B, et al. Prevalence and molecular characterization of extended spectrum β -Lactamase and carbapenemase-producing *Enterobacteriaceae* isolates from bloodstream infection suspected patients in Addis Ababa, Ethiopia. *Infection and Drug Resistance*. 2022:1367-82.
8. Sewunet T, Asrat D, Woldeamanuel Y, Aseffa A and Giske CG. Molecular epidemiology and antimicrobial susceptibility of *Pseudomonas* spp. and *Acinetobacter* spp. from clinical samples at Jimma medical center, Ethiopia. *Frontiers in microbiology*. 2022;13:951857.
9. Legese MH, Asrat D, Mihret A, Hasan B, Mekasha A, Aseffa A, et al. Genomic epidemiology of Carbapenemase-producing and Colistin-resistant *Enterobacteriaceae* among Sepsis patients in Ethiopia: a whole-genome analysis. *Antimicrobial agents and chemotherapy*. 2022;66(8):e00534-22.
10. Awoke T, Teka B, Aseffa A, Sebre S, Seman A, Yeshitela B, et al. Detection of bla KPC and bla NDM carbapenemase genes among *Klebsiella pneumoniae* isolates in Addis Ababa, Ethiopia: Dominance of bla NDM. *PLoS One*. 2022;17(4):e0267657.

Common chest radiographic patterns and associated factors of among drug-resistant tuberculosis patients at the University of Gondar Comprehensive Specialized Hospital, Northwest Ethiopia, 2020

Samuel Addis Mihiretie¹, Temesgen Tadesse Alemayehu*¹, Tewodros Tsegaye Ayele², Getahun Molla Kassa^{3,4}

¹Department of Radiology, School of Medicine, College of Medicine and Health Science, University of Gondar, Gondar, Ethiopia, ²Department of Internal Medicine, School of Medicine, College of Medicine and Health Science, University of Gondar, Gondar, Ethiopia, ³Department of Epidemiology and Biostatistics, Institute of Public Health, College of Medicine and Health Science, University of Gondar, Gondar, Ethiopia, ⁴Population Health Sciences, Bristol Medical School, University of Bristol, Bristol, United Kingdom.

*Corresponding author: email: tomtadesse@gmail.com

Citation: Mihiretie SA, Tadesse T, Ayele TT, Kassa GM. Common chest radiographic patterns and extensive disease among adult pulmonary drug resistant tuberculosis patients at the University of Gondar Comprehensive Specialized Hospital, Northwest Ethiopia. *Ethiop J Health Biomed Sci* 2024;14(2):3-11.

DOI: <https://doi.org/10.20372/ejhs.v14i2.855>

Article History

Received: July 15, 2024

Revised: November 15, 2024

Published: December 31, 2024

Keywords: drug-resistant tuberculosis, chest radiograph, advanced tuberculosis disease

Publisher: University of Gondar

Abstract

Background: Drug-Resistant Tuberculosis (DR-TB) is a multifaceted public health problem. Determining the common chest radiographic patterns, degree of lung damage, and associated factors is vital in the early detection and treatment of DR-TB. Despite the availability of x ray, there are gaps in chest radiographic patterns of DR-TB disease in Ethiopia.

Objectives: This study aimed to identify common radiologic patterns among pulmonary DR-TB patients.

Method: A hospital-based cross-sectional study was conducted among 182 DR-TB patients who had an archive of baseline chest radiographs at the University of Gondar Comprehensive Specialized Hospital from September 2010 to October 2020. The socio-demographic and radiographic patterns were depicted using descriptive statistics. A multivariable binary logistic regression model was applied to identify associated variables with extensive DR-TB diseases at a $p < 0.05$.

Result: Out of 182 DR-TB patients, 112 (61.54%) had patchy consolidation followed by focal fibrotic changes (37.91%) and focal nodular opacities (26.92%). Of all DR-TB patients, 19% had extensive pulmonary DR-TB disease. Patients' marital status was significantly associated with extensive (advanced) DR-TB disease. The odds of having advanced TB disease were 0.15 among those with single marital status (AOR: 0.15, 95% CI: 0.03, 0.68).

Conclusion: This study highlighted that the most common chest radiographic feature of DR-TB was patchy consolidation followed by fibrosis and focal nodular opacities. Additionally, the study showed that close to one out of five DR-TB patients had extensive (advanced) DR-TB disease. Marital status had a significant association with extensive (advanced) DR-TB disease.

Copyright: © 2024 at Mihiretie et al. This is an open access article distributed under the terms of the Creative Commons Attribution-NonCommercial 4.0 (CC BY NC 4.0) License, which permits unrestricted use, distribution, and reproduction in any medium, provided the original author and source are credited.

Introduction

Public health in resource-limited countries and the Tuberculosis (TB) Elimination Program are endangered by the emergence of drug-resistance tuberculosis (DR-TB). Disease management is difficult given the difficulty of diagnosis, complexity of treatment, deep adverse drug events and drug cost, high disease burden, and limited access to well-equipped health care facilities (1, 2). Tuberculosis is the leading cause of death in the world among infectious diseases (3, 4). If treatment is not initiated soon after diagnosis, a person with TB disease may infect an average of 10–15 other people every year (5).

Ethiopia is one of the 30 countries with a high burden of TB, TB/HIV, and DR-TB, with an annual estimated incidence of 177 per 100,000 carrying drug-susceptible TB (6). In addition, the burden of DR-TB reported among TB patients in Ethiopia is increasing from time to time (7, 8).

Diagnosis of DR TB relies on both laboratory studies (acid-fast staining, cultures, and different molecular tests) and imaging modalities including x-ray. Despite confirmative diagnosis of TB and DR-TB, early suspicions of DR-TB by chest imaging are highly desirable to guide the diagnostic process (9). Chest radiograph plays a major role in the detection, screening, and surveillance of DR TB as it is widely available and cheap (10). It can generally enable detection of different morphologies of lesions such as nodules, cavities, consolidation, fibrotic and bronchiectatic changes, pleural effusion, and thickening, as well as the site of involvement and number of lesions. It can also help in the follow-up of TB patients' treatment response (11). Despite the relatively low sensitivity and specificity of plain chest radiography, it is very helpful and commonly used in planning the management of complicated TB including DR-TB. Moreover, chest radiography entails reduced radiation exposure and affordable cost compared with Computer Tomography (CT) scans (18).

Radiological manifestations of pulmonary tuberculosis depend on several host factors that include prior exposure to TB, age, and underlying immune status. In people with normal immune function, radiological manifestations can be logically divided into two different forms of primary and post-primary disease that develop in individuals with and without prior TB exposure (12). Primary DR-TB chest radiographic patterns resem-

ble those of primary drug-susceptible TB features, like consolidation and pleural effusion. On the other hand, secondary DR TB presents as an imaging feature of reactivation TB and cavitary consolidation (13, 14). In immunocompromised cases like Human Immunodeficiency Virus (HIV) positive DR-TB patients, hilar and mediastinal lymphadenopathies and miliary spread were the most common chest radiographic findings (1).

As the burden of DR- TB is high in Ethiopia, familiarity with the radiographic patterns of DR-TB can enable early detection, recognition, and treatment follow-up of the DR-TB disease. In addition, knowing the prevalence and associated factors for extensive (advanced) DR-TB disease will help the treating health care workers to quickly triage and implement patient-centered care. Despite the value of chest radiography in early detection and, follow-up, there has been no study of chest radiographic patterns of DR-TB disease in Ethiopia to date. This research aimed to explore the common radiological findings, the proportion of extensive disease, and associated factors among confirmed pulmonary DR-TB patients at the University of Gondar Comprehensive specialized hospital, Northwest Ethiopia.

Method

Study design, period, and setting

An institution-based cross-sectional study was conducted to determine common chest radiographic patterns and associated factors of drug resistant tuberculosis disease among DR-TB patients from November 01, 2020 to February 20, 2021. The study was done in the DR-TB treatment center at the University of Gondar Comprehensive Specialized Hospital with eligible patients admitted between September 2010 to October 2020. At the hospital, DR-TB treatment is based on the recommendations of the Ethiopian Federal Ministry of Health National DR-TB Guidelines, which are based on recommendations from WHO guidelines. Eligible patients should have at least bacteriological evidence of rifampicin resistance (RR-TB) confirmed by Gene Xpert/MTB-RIF, a Line Probe Assay, culture and drug sensitivity tests, the clinical judgment of the DR-TB clinical panel team based on multiple treatment failures, or a history of contact with someone having DR-TB. All the DR-TB patients in the hospital have a baseline chest x-ray film before initiating second-line anti-TB treatment. In the Department of Medical Imaging, the hospital has multimodal

imaging instruments including radiography (previously analog now replaced by digital), ultrasound, CT, and Magnetic Resonance Imaging (MRI).

Source and study population

The source population of this study was comprised of all adult (above 18 years old) DR-TB patients who registered and started second-line DR-TB treatment at the University of Gondar Comprehensive Specialized Hospital from September 2010 to October 2020. The study population consisted of those pulmonary DR-TB patients who had a documented baseline chest radiograph and started treatment at University of Gondar Comprehensive Specialized-Hospital.

Sample size and sampling procedures

All pulmonary DR-TB patients who were treated at the University of Gondar Comprehensive Specialized Hospital DR-TB clinic within the study period and have documented baseline chest radiographic films were included in this study.

Inclusion and exclusion criteria

All confirmed adult pulmonary DR-TB patients with at least one chest radiograph from their baseline evaluation were initially included in this study, but those with poor quality chest radiographs for which interpretation was difficult were ultimately excluded. The total number of DR-TB patients included in the study was 182. Data was collected by a final year radiology resident and a senior radiologist confirmed the quality of radiographs and interpretations.

Variable of the study

The dependent variable in this study was extensive (advanced) DR-TB disease measured as the presence or absence of any of the following: bilateral cavitory lung lesions, extensive parenchymal damage, diffuse chronic changes, multi-lobar consolidation, diffuse nodular opacities, or diffuse patchy consolidations and military nodules on chest radiograph (WHO operational definition) (15).

Cavity: is a gas-filled space surrounded by a complete wall that is three millimeters or greater in thickness.

Consolidation: is homogenous, ill-defined, or fluffy opacity that obscures vessels having air bronchograms with preserved lung volume and bounded by a fissure.

Pleural effusion: is homogenous increased lower lung zone opacity in the lateral costophrenic sulcus with concave interface towards the lung (meniscus sign).

Infiltrates: are reticulonodular lesions; a combination of reticular and nodular lesions.

Hilar lymphadenopathy: is considered when there is hilar enlargement, increased hilar density, lobulations of the contour, and distortion of the main bronchi.

Fibrotic changes: are old pleural and pulmonary scars, thin linear shadows with pleural thickening, and tenting of the diaphragm when these shadows extend to the pleural surface.

Bronchiectasis: refers to parallel linear shadows representing walls of cylindrically dilated bronchi seen in length and multiple peripherally located thin-walled cysts that tend to cluster in the distribution of the bronchovascular bundle. The explanatory variables in this study were sex, age, residence, occupation, religion, educational status, cigarette smoking history, alcohol drinking history, number of previous TB treatment cycles, baseline sputum smear results, baseline sputum smear grading, co-morbidities, and nutritional status.

Data collection procedures

After ethical approval, medical charts were collected from the DR-TB clinic and patient information was collected from charts. Chest radiographic findings were interpreted from the attached radiographs by a radiologist and recorded. Data completeness was verified each day.

Data processing and analysis

The collected data was entered into Epi-data 4.6.0.0 and exported to SPSS version 20 statistical software for cleaning, coding, recoding, and analysis. Descriptive statistics were derived for frequency and percent for categorical variables, means with Standard Deviation (SD) and presented in texts, tables, and graphs. COR and AOR were assessed to identify the associated factors of extensive (advanced) DR-TB at $p < 0.05$. Model fitness was assessed by using the Hosmer and Lemeshow test and reported adequate when $p > 0.05$.

Result

Socio-demographic and clinical characteristics

In this study, a total of 182 DR-TB patients were included, of which 109 were males. Age ranged from 18 - 73 years with a mean and standard deviation (SD) of 34.32 ± 0.89 years. All patients had been previously treated for TB at least once (all are secondary DR-TB). Of the total, 74.72% of patients had a documented positive baseline sputum smear result. A quarter of patients, 47 (25.3%) were HIV co-infected:- of these, only 28 had CD4 counts at the start of DR-TB treatment (**Table 1**).

Table 1: Socio-demographic and clinical characteristics of DR-TB patients at the University of Gondar Comprehensive Specialized Hospital (N=184), September 2010 to October 2020.

Variables	Category	Extensive (advanced) DR-TB Disease			
		Yes	No	Total	Percentage
Sex	Male	17	92	109	59.89%
	Female	14	59	73	40.10%
Age in years	18-44 years	28	114	142	78.02%
	45-64 years	7	29	36	19.78%
	≥ 65 years	0	4	4	2.19%
Residency	Urban	14	58	72	39.56%
	Rural	21	87	108	59.34%
Occupation	Unemployed	34	137	171	93.95%
	Employed	1	8	9	4.94%
Religion	Orthodox	33	136	169	92.85%
	Muslim	2	9	11	6.04%
Educational status	Primary & below	24	98	122	67.03%
	Secondary & above	9	33	42	23.07%
Marital status	Married	19	52	71	39.01%
	Never married	6	56	62	34.06%
	Divorced & widowed	10	39	49	26.92%
Cigarettes smoking history	Yes	1	13	14	7.69%
	No	34	134	168	92.30%
Alcohol drinking history	Yes	0	10	10	5.49%
	No	35	137	172	94.50%
History of TB treatment in number	≤ one	24	102	126	69.23%
	> one	11	45	56	30.79%
Anatomical site of DR-TB affected	Only pulmonary	26	121	147	80.76%
	Disseminated	9	26	35	19.23%
Baseline sputum smear result	Positive	25	111	136	74.72%
	Negative	10	32	42	23.07%
Baseline sputum smear grading	No bacilli (0)	10	32	42	23.07%
	Scanty +1	10	47	57	31.31%
	+2 and 3+	13	55	68	37.36%
Co-morbid conditions	Diabetic mellitus	0	4	4	2.19%
	CVD	0	2	2	1.09%
	HIV	10	37	47	25.82%
Have the patient started ART (N=47)	Yes	9	34	43	23.62%
	No	1	3	4	2.19%
CD4 count at the start of DR-TB treatment (cells/mm ³) (N=28)	≤ 50	1	2	3	1.64%
	51-100	1	2	3	1.64%
	101-200	2	7	9	4.94%
	>200	1	12	13	7.14%

* CVD (Cardiovascular Disorders), HIV (Human Immunodeficiency Virus), ART (Anti-retro Viral Therapy), CD4 (Cluster of Differentiation 4), mm (millimeter)

Radiologic pattern and prevalence of extensive (advanced) DR-TB

Of all 182 DR-TB patients, 61.54% patients had patchy consolidation, 37.91% had focal fibrotic changes and 26.92% of them had focal nodular opacities (**Figure 1**). In those patients with a single cavity, the mean and SD cavity diameter was

3.27 ± 0.23 cm. The smallest cavity had a diameter of 1.0 cm and the largest had 6.0 cm. Among those DR-TB patients who had multiple cavities, the mean and SD diameter size was 4.22 ± 1.47cm with the smallest and largest cavity size of 2.0 cm and 6.0 cm diameter respectively.

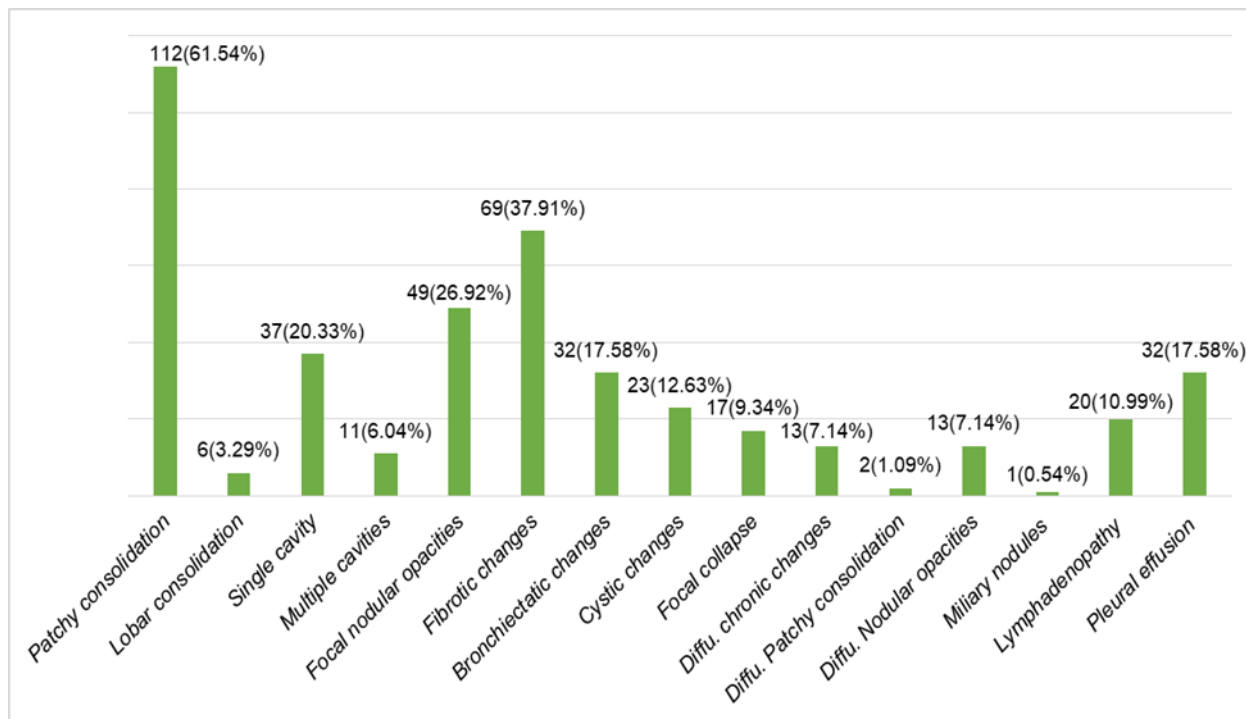


Figure 1: Radiographic findings of DR-TB patients at the University of Gondar Comprehensive Specialized Hospital (N=184), September 2010 to October 2020.

The prevalence of advanced DR-TB disease was 19% (95% CI: 13, 25). Of those patients with extensive (advanced) DR-TB, 13 (7.14%) had diffuse chronic changes, 13 (7.14%) had diffuse nodular opacities, 11 (6.04%) had multiple cavities, 3 (1.65%) had bilateral cavities, 2 (1.10%) had diffuse patchy consolidation and only one (0.55%) patient had miliary nodules. There was no patient with multi-lobar consolidation.

The common findings in the chest radiograph were patchy consolidation 112 (61.54%) followed by focal fibrotic chronic changes 69 (37.91%), focal nodular opacities 49 (26.92%), and single cavity 37 (20.33%) respectively. The right and left upper lung zones were the most affected anatomical sites by DR-TB (**Table 2**).

Table 2: Radiological findings of DR-TB patients at the University of Gondar Comprehensive Specialized Hospital (N=184), September 2010 to October 2020.

Findings	No. of patients	Right upper zone	Right middle zone	Right lower zone	Left upper zone	Left middle zone	Left lower zone
Patchy consolidation	112	51	26	15	45	18	14
Lobar consolidation	6	1	1	1	1	2	1
Single cavity	37	12	7	0	14	2	2
Multiple cavities	11	6	2	1	4	6	2
Focal nodular opacities	49	26	12	0	21	12	7
Focal chronic changes (fibrosis)	69	38	10	0	35	6	4
Focal chronic changes (bronchiectasis)	32	14	5	1	23	6	3
Focal chronic changes (cysts)	23	12	3	3	10	5	3
Focal chronic changes (collapse)	17	7	2	0	7	2	3

Associated factors for extensive (advanced) DR-TB disease

In this study, we have assessed the association between extensive (advanced) DR-TB disease and socio-demographic, behavioral, and clinical characteristics. From the chi-square test, sex, marital status, educational level, residency, previous TB treatment history, anatomical site of DR-TB involvement, baseline sputum smear results, baseline sputum culture re-

sults, co-morbidity, and baseline sputum grading satisfied the assumption and fitted in the multivariable binary logistic regression model. We used the backward logistic regression selection method to identify those variables that were significantly associated with extensive (advanced) DR-TB disease at a p-value of <0.05. From the multivariable binary logistic regression model, only marital status was significantly associated with extensive (advanced) DR-TB disease. (**Table 3**).

Table 3: Multivariable binary logistic regression of DR-TB patients at the University of Gondar Comprehensive Specialized Hospital (N=184), September 2010 to October 2020.

Variables	Category	Extensive (Advanced) DR-TB Disease		AOR(95% CI)	P. value
		Yes	No		
Sex	Male	17	92	0.38 (0.15, 0.98)	0.045
	Female	14	59	1	
Age in years	Mean \pm SD	33.6 \pm 9.9	34.46 \pm 12.52	0.99 (0.94, 1.04)	
Marital status	Married	19	52	1	0.018
	Never married	6	56	0.96 (0.34,2.75)	
	Divorced & widowed	10	39	0.17 (0.94,0.74)	
Residency	Urban	14	58	0.62 (0.23,1.66)	0.34
	Rural	21	87	1	
Educational status	Primary & below	24	98	0.66 (0.20,2.22)	0.51
	Secondary & above	9	33	1	
Co-morbidity disease	Yes	10	45	1	0.57
	No	25	102	1.34 (0.49,3.66)	
Previous TB treatment history	\leq 1	24	102	2.98 (0.94,9.45)	0.064
	>1	11	45	1	
Site of TB	pulmonary only	26	121	1	0.48
	Disseminated	9	26	0.67 (0.22,2.05)	
Baseline sputum culture	Positive	19	95	1	0.45
	Negative	9	32	0.67(0.24,1.90)	
Co morbidity	Yes	10	45	1	0.57
	No	25	102	1.34(0.49,3.66)	
Smear grading	No bacilli	10	32	1	0.77
	Scanty & +1	10	47	1.19(0.37,3.84)	
	+2 & +3	13	55	1.46(0.51,4.13)	

Hosmer and Lemeshow test (p-value=0.78), AOR (Adjusted Odds Ratio), CI (Confidence Interval), TB (Tuberculosis), SD (Standard Deviation)

Discussion

In this study, the four most common radiological findings were patchy consolidation (61.54%), fibrotic changes (37.91%), focal nodular opacities (26.92%), and single cavity (20.33%). Out of 182 patients included in this study, 118 patients had consolidation (either patchy or lobar), which

was predominantly found on the right and left upper lung zones accounting for 52 (44.06%) and 46 (38.93%) cases respectively. Those zonal distributions, bilateralism, and preference towards the upper lung zones were noted similarly in studies done in Indonesia and Iran (11, 16). Even though consolidation was the most prevalent finding in our study, it was lower than study reports from Indonesia and Iran (11, 16). This difference might be due to the smaller

sample size or repeated TB treatments where the prevalence of fibrotic lung was higher and may lower the proportion of consolidation. Additionally, the long delay time in the diagnosis and initiation of treatment may result in ongoing chronic inflammation and as a result, causing fibrosis of the lung to be the second most common imaging feature in our cases. One can also consider the late presentation of our patients as a factor in the disease process that culminates in pulmonary fibrosis. The treatment failure rate in our country is high compared with that in other countries and several patients are subjected to repeated treatment. Moreover, cultures are done in only a few centers and most patients are subjected to repeated treatment with conventional anti-tuberculosis drugs if they do not respond to the initial treatment.

The prevalence of hilar lymphadenopathy (LAP) (10.99%) was lower than in the report from Iran (16). The reason behind this discrepancy might be the use of highly sensitive imaging like CT or digital x-ray which was not routinely taken for all of our patients.

Of all 182 adult DR-TB patients in this study, 19% had extensive (advanced) disease. Of those with extensive (advanced) DR-TB disease, diffuse chronic changes and diffuse nodular opacities were the dominant findings. This might be due to late presentations and/or due to repeated exposure to conventional anti-TB regimens before the diagnosis of DR-TB. Multiple cavities were the third main findings following diffuse chronic changes and diffuse nodular opacities. But multiple cavities were less prevalent compared with other studies which showed multiple cavities were common radiological findings (9, 17). Based on the 2020 WHO and Ministry of Health Ethiopia PMDT guideline, DR-TB patients with extensive (advanced) disease are not eligible for the shorter all-oral bedaquiline containing regimen. This implies that nearly one out of five DR-TB patients in this study were not eligible to benefit from this regimen. This short regimen is expected to reduce the duration of treatment from 18 or more months to 9-12 months, decreasing the rate of patients lost to follow-up, increase successful treatment outcomes, and improve programmatic including drug supplies and procurements than longer regimens (15, 18, 19).

In this study, the chest radiographic pattern among HIV positive and HIV negative DR-TB patients was similar. Only 28 HIV-positive patients had CD4 counts at the time of DR-TB diagnosis and we could not, therefore, evaluate imaging at

different CD4 values. Lack of CD4 count was also seen in a study done in Alert hospital, Addis Ababa, Ethiopia (21).

Limitation: The inability to find an adequate number of patients, incompleteness of data, and poor quality x-ray film were the primary constraints for this study.

Conclusions and recommendation: This study highlighted that one out of five pulmonary DR-TB patients (19%) has extensive (advanced) DR-TB disease. Fibrotic changes and patchy consolidations are the most common findings on chest x-ray. Marital status had a significant association with extensive (advanced) DR-TB disease.

Hilar lymphadenopathy was not common finding in our study compared with other previous studies so additional use of routine lateral chest x-ray in addition to posteroanterior chest radiograph may increase the detection rate of lymphadenopathy.

Abbreviations: Drug-Resistant Tuberculosis (DR-TB), Tuberculosis (TB), Multidrug-Resistant Tuberculosis (MDR-TB), *Mycobacterium Tuberculosis* Rifampicin-Resistant (MTB-RIF), World Health Organization (WHO), Adjusted Odds Ratio (AOR), Confidence Interval (CI), Interquartile Range (IQR), Standard Deviation (SD), Acquired Immune-Deficiency Syndrome (AIDS), Human Immunodeficiency Virus (HIV), Computer Tomography (CT), and Magnetic Resonance Imaging (MRI), Rifampicin Resistance (RR-TB).

Competing interests: The authors have declared that there is no conflict of interest in this study.

Data availability: The data used for the current study was available based on a reasonable request from the lead author.

Ethical considerations: Ethical approval was obtained from the Institutional Review committee of the University of Gondar. A letter granting permission to conduct the study was secured from the Chief Clinical Director of the University of Gondar Comprehensive Specialized Hospital and the head of the DR-TB clinic. Confidentiality was ensured by omitting personal identifiers.

Consent for publication: Not applicable.

Funding: This study had funding for the data collection from the University of Gondar to compensate the post-graduate student.

Authors' contributions: All authors: selected the title, analyzed the data, conceptualizing the discussion, prepared and

approved the manuscript. SAM and TTA: developed the proposal. SAM, GMK, and TTA: followed the data quality. SAM and GMK: wrote the methods section of the manuscript.

Acknowledgment

We would like to express our thanks to the University of Gondar Comprehensive Specialized Hospital for permitting us to conduct this research. We especially thank the DR-TB treatment center staff and data collectors for their contributions to the success of this research article.

Author information: Samuel Addis Mihiretie (MD, Radiologist at the University of Gondar), Temesgen Tadesse Alemayehu (MD, Assistance Professor of Radiology at the University of Gondar), Tewodros Tsegaye Ayele (Assistance professor of Medicine, MPH, MD), and Getahun Molla Kassa (Lecturer at the University of Gondar, MPH in Epidemiology and Biostatistics, MSc in Clinical Tropical Infectious Diseases and HIV Medicine).

Reference

1. Lee ES, Park CM, Goo JM, Yim J-J, Kim H-R, Lee HJ, et al. Computed tomography features of extensively drug-resistant pulmonary tuberculosis in non-HIV-infected patients. *Journal of computer assisted tomography*. 2010;34(4):559-63.
2. Harries AD, Kumar A. Challenges and progress with diagnosing pulmonary tuberculosis in low-and middle-income countries. *Diagnostics*. 2018;8(4):78.
3. World Health Organization. *Global Tuberculosis Report*. Geneva: World Health Organization; 2014. Contract No: WHO/HTM/TB. 2016.
4. World Health Organization. *Global Tuberculosis Report*. Geneva: 2020.
5. Dye C, Lönnroth K, Jaramillo E, Williams B, Raviglione M. Trends in tuberculosis incidence and their determinants in 134 countries. *Bulletin of the World Health Organization*. 2009;87:683-91.
6. FMOH E. *Guidelines for management of TB, DR-TB and leprosy in Ethiopia*. Addis Ababa, Ethiopia Federal Ministry of Health Ethiopia. 2017.
7. Sinshaw W, Kebede A, Bitew A, Tesfaye E, Tadesse M, Mehamed Z, et al. Prevalence of tuberculosis, multidrug resistant tuberculosis and associated risk factors among smear negative presumptive pulmonary tuberculosis patients in Addis Ababa, Ethiopia. *BMC infectious diseases*. 2019;19(1):641.
8. Girum T, Muktar E, Lentiro K, Wondiye H, Shewangi-zaw M. Epidemiology of multidrug-resistant tuberculosis (MDR-TB) in Ethiopia: a systematic review and meta-analysis of the prevalence, determinants and treatment outcome. *Tropical diseases, travel medicine and vaccines*. 2018;4(1):5.
9. Wáng YXJ, Chung MJ, Skrahin A, Rosenthal A, Gabrielian A, Tartakovsky M. Radiological signs associated with pulmonary multi-drug resistant tuberculosis: an analysis of published evidences. *Quantitative imaging in medicine and surgery*. 2018;8(2):161.
10. Jaeger S, Juarez-Espinosa OH, Candemir S, Poostchi M, Yang F, Kim L, et al. Detecting drug-resistant tuberculosis in chest radiographs. *International journal of computer assisted radiology and surgery*. 2018;13(12):1915-25.
11. Icksan AG, Napitupulu MRS, Nawas MA, Nurwidya F. Chest X-ray findings comparison between multi-drug-resistant tuberculosis and drug-sensitive tuberculosis. *Journal of natural science, biology, and medicine*. 2018;9(1):42.
12. Karimi M, Arvin S, Bazari RAM, editors. *Computed tomography features of multidrug-resistant tuberculosis (MDR TB) in HIV+ patients 2015: European Congress of Radiology 2015*.
13. Fishman JE, Sais GJ, Schwartz DS, Otten J. Radiographic findings and patterns in multidrug-resistant tuberculosis. *Journal of thoracic imaging*. 1998;13(1):65.
14. Kahkouee S, Esmi E, Moghadam A, Karam MB, Mosadegh L, Salek S, et al. Multidrug resistant tuberculosis versus non-tuberculous mycobacterial infections: a CT-scan challenge. *The Brazilian journal of infectious diseases : an official publication of the Brazilian Society of Infectious Diseases*. 2013;17(2):137-42.
15. World Health Organization. *WHO operational handbook on tuberculosis. Module 4: treatment - drug-resistant tuberculosis treatment*. Geneva 2020.

16. Zahirifard S, Amiri M, Bakhshayesh KM, MIRSAEIDI SM, Ehsanpour A, Masjedi M. The radiological spectrum of pulmonary multidrug-resistant tuberculosis in HIV-negative patients. 2003.
17. Kim S, Min J, Lee J. Radiological findings of primary multidrug-resistant pulmonary tuberculosis in HIV-seronegative patients. *Hong Kong J Radiol.* 2014;17(1):4-8.
18. World Health Organization. WHO consolidated guidelines on drug-resistant tuberculosis treatment. Geneva: World Health Organization; 2019. Licence: CC BY-NC-SA 3.0 IGO. . 2019.
19. Ministry of Health-Ethiopia. National Programmatic Management of Drug-resistant TB (PMDT) in Ethiopia. Addis Abeba.2019.
20. Krishnan L, Akande T, Shankar AV, McIntire KN, Gounder CR, Gupta A, et al. Gender-related barriers and delays in accessing tuberculosis diagnostic and treatment services: a systematic review of qualitative studies. *Tuberculosis research and treatment.* 2014;2014.
21. Legesse tK. Chest radiographic pattern of multidrug resistance (MDR) tuberculosis cases at alert hospital, Addis Ababa A retrospective cross sectional study. 2019.

Antioxidant Activity Of The Leaf Extracts of *Boscia coriacea* Graells And *Uvaria leptocladon* Oliv

Sintayehu Tsegaye Tseha^{1*}, Yalemtehay Mekonnen², Asnake Desalegn³, Mesfin Getachew⁴, Paulos Getachew⁵, Melaku Wondafarsh⁶

¹ Department of Biology, Collage of Natural and Computational Sciences, Arba Minch University, Arba Minch, Ethiopia, ²Department of Zoological Sciences, College of Natural and Computational Sciences, Addis Ababa University, Addis Ababa, Ethiopia, ³ Department of Microbial, Cellular and Molecular Biology, College of Natural and Computational Sciences, Addis Ababa University, Addis Ababa, Ethiopia, ⁴Department of Industrial Chemistry, College of Applied Sciences, Addis Ababa Science and Technology University, Ethiopia, ⁵Center for Food Science and Nutrition, College of Natural and Computational Sciences, Addis Ababa University, Addis Ababa, Ethiopia, ⁶Department of Plant Biology and Biodiversity Management, College of Natural and Computational Sciences, Addis Ababa University, Addis Ababa, Ethiopia.

*Corresponding author: email: sintayehu.tsegaye@amu.edu.et and sintayehutsegaye783@gmail.com

Citation: Tseha S, Mekonnen Y, Desalegn A, Tadesse M, Getachew P, Wondafarsh M. Antioxidant activity of the leaves extracts of *Boscia coriacea* Graells and *Uvaria leptocladon* Oliv. Ethiop J Health Biomed Sci 2024;14(2):13-22.

DOI: <https://doi.org/10.20372/ejhs.v14i2.886>

Article History

Received: August 30, 2024

Revised: November 25, 2024

Published: December 31, 2024

Key words: *Boscia coriacea* Graells, *Uvaria leptocladon* Oliv, antioxidant activity, DPPH, ABTS, FRAP, phenol content, flavonoid content

Publisher: University of Gondar

Abstract

Background: Synthetic antioxidants used for the management of oxidative stress have been shown to have severe side effects. Some medicinal plants that belong to the genus *Uvaria* and *Boscia* contain chemicals with antioxidant properties such as flavonoids and alkaloids.

Objective: This study was aimed to evaluate the antioxidant activities of the leaf extracts of *Boscia coriacea* Graells and *Uvaria leptocladon* Oliv.

Method: Fresh leaves of *B. coriacea* and *U. leptocladon* were collected in April 2021 from Alie and Konso, located in Southern Ethiopia. First, the leaves of the medicinal plants were dried in dark conditions. Maceration extraction method was used to extract the powdered leaf of *Boscia coriacea* and *Uvaria leptocladon*. The crude extract of *B. coriacea* was fractionated using chloroform (CHCl_3), methanol (CH_3OH), CHCl_3 : CH_3OH (1:1 v/v) and petroleum ether. The crude extract of *U. leptocladon* was fractionated using CHCl_3 , ethanol ($\text{C}_2\text{H}_6\text{OH}$), and ethyl acetate ($\text{C}_4\text{H}_8\text{O}_2$). Evaluation of the antioxidant activity was done using 2,2-diphenyl-1-picrylhydrazyl (DPPH), 2,2'-azinobis-(3-ethylbenzothiazoline-6-sulfonic acid (ABTS), and ferric reducing antioxidant power (FRAP) assays. Data analysis was done using one-way analysis of variance.

Result: The antioxidant evaluation demonstrated that the leaf extracts of *B. coriacea* and *U. leptocladon* have 2,2-diphenyl-1-picrylhydrazyl and 2,2'-azinobis-(3-ethylbenzothiazoline-6-sulfonic acid radical scavenging activity. Based on IC_{50} value, the CH_3OH : CHCl_3 (1:1) fraction of *B. coriacea* (IC_{50} =38.2 $\mu\text{g}/\text{mL}$) and the $\text{C}_2\text{H}_6\text{OH}$ fraction of *U. leptocladon* (IC_{50} =30.5 $\mu\text{g}/\text{mL}$) are highly active in 2,2-diphenyl-1-picrylhydrazyl free radical scavenging activity. The total flavonoid content in the CH_3OH : CHCl_3 fraction of *B.coricea* and in the $\text{C}_2\text{H}_6\text{OH}$ fraction of *U.leptocladon* were calculated to be 136.8 \pm 0.04 mg/g of extract and 172.9 \pm 0.41 mg/g of extract, respectively. The total phenol content in the CH_3OH : CHCl_3 fraction of *B.coricea* and in the $\text{C}_2\text{H}_6\text{OH}$ fraction of *U.leptocladon* were calculated to be 145 \pm 0.025 mg/g and 187.7 \pm 0.055 mg/g, respectively. The CH_3OH : CHCl_3 (1:1) fraction of *B. coriacea* and the $\text{C}_2\text{H}_6\text{OH}$ fraction of *U. leptocladon* showed the highest ferric reducing antioxidant power. The antioxidant effects of the leaf extract of *B. coriacea* are due to β -sitosterol and lucidine-type compound. The antioxidant effects of the leaf extract of *U. leptocladon* are attributed to β -sitosterol, β -sitosterol glucoside, and α -humulene.

Conclusion: The leaf extracts of *B. coriacea* and *U. leptocladon* have high antioxidant activity. Further study is needed to determine the mechanism of action of compounds isolated from the leaf extracts of *B. coriacea* and *U. leptocladon*.

Introduction

Oxidative stress refers to condition when an imbalance occurs between formations of free radicals and antioxidants (1). Several studies demonstrated that that oxidative stress can be involved in the onset and/or progression of several diseases (i.e., cancer, diabetes, metabolic disorders, atherosclerosis, and cardiovascular disease (2)). A free radical is a molecule which possesses an unpaired electron that makes it unstable. The unstable free radicals become stable when electron pairing occurs with biological macromolecules such as proteins and lipids, in healthy human cells (3). Antioxidants are chemicals that prevent and stabilize the damage caused by free radicals by supplying electrons and converting them into waste by-products (3). Synthetic antioxidants that are used for the management of oxidative stress have been shown to have severe side effects (4). For this reason, searching for safe and effective natural antioxidants is needed.

Medicinal plants are major sources of chemicals with bioactive compounds. Some medicinal plants that belong to the genus *Uvaria* and *Boscia* have antioxidant properties (5, 6). The commonly mentioned phytochemicals that are found in leaf extracts of plants that belongs to the genus *Boscia* include flavonoids, alkaloids, saponins, steroids, and cardiac glycosides (6-9). The major phytochemicals in the leaf extracts of *Uvaria* species include: phenol, steroid, alkaloids, saponins, flavonoids and terpenoids (9-14).

The genus *Boscia* belongs to the family Cappariaceae and the genus *Uvaria* belongs to the family Annonaceae, which are widely distributed in Ethiopia (15). For instance *Boscia coriacea* is found in Bale, Sidamo, Kefa, Konso, Gamo Gofa and Hararge regions of Ethiopia. *Uvaria leptocladon* is found in Sidamo, Kefa, Konso (Alie), and Gamo Gofa regions of Ethiopia (15). Thus, the objective of this study was to evaluate the antioxidant activities of the leaf extracts of *B. coriacea* Graells and *U. leptocladon* Oliv.

Material and Method

Plant collection

Fresh leaves of *B. coriacea* and *U. leptocladon* were collected from Konso and Alie, located in the Southern Nation, Nation-

alities, and People Region, Ethiopia, in April 2021. The plant materials were authenticated by one of the authors of this manuscript (Mr. Melaku Wondafrash a Botanist at the Department of Plant Biology and Biodiversity Management, Addis Ababa University), and a voucher specimen of each plant (ST001 and ST002, representing *B. coriacea* and *U. leptocladon*, respectively) was deposited at the National Herbarium, College of Natural and Computational Sciences, Addis Ababa University (AAU).

Extraction

First, the leaves of the plants dried in dark condition. Then, the extraction of the powdered leaf of *B. coriacea* (1 kg) and *U. leptocladon* (1 kg) was done using 10 liters of 80% methanol by maceration extraction method. Filtration of the mixture was performed using Whatmann no.1 filter paper. Rotary evaporator (PHOENIX instrument, RE-100D) was used to evaporate the CH₃OH from the filtrate. A lyophilizer equipment (Christ, ALPHA 2-4-LD plus, Germany) was used to remove the water component of the mixture.

The crude leaf extracts of the two plants were fractionated in the Department of Chemistry, CNCS, AAU. The crude extract of *B. coriacea* was fractionated using chloroform (CHCl₃), methanol (CH₃OH), CHCl₃: CH₃OH (1:1 v/v) and petroleum ether. The crude extract of *U. leptocladon*, was fractionated using CHCl₃, ethanol (C₂H₆OH), and ethyl acetate (C₄H₈O₂). All the extracts were stored at -20°C until the experiments were conducted. The isolation and characterization of compounds were done at the Department of Chemistry, CNCS, AAU. The characterization of compounds was done using nuclear magnetic resonance spectrometry (1H NMR and 13C NMR).

2, 2-diphenyl-1-picrylhydrazyl (DPPH) radical scavenging assay

The 2, 2-diphenyl-1-picrylhydrazyl (DPPH) radical scavenging assay was carried out according to Brand-Williams et al (1995) (16) and Molyneux (2004) (17) with modification.

Stock solutions of the plant extracts, 1mg/mL diluted to different concentrations ranging from 0.02 to 0.20 mg/mL (0.02, 0.04, 0.08, 0.12, 0.16 and 0.20 mg/mL). Five mL of 1 mM DPPH in CH₃OH was added to the different concentrations of extracts. Then, the mixture was shaken and allowed to stand in dark condition. After 30 minutes, absorbance was read at 517 nm against a blank containing CH₃OH using spectrophotome-

ter (UV-UV/Vis/NIR spectrophotometer, Perkin Elemer, Lambda 950). Ascorbic acid was used as positive control with similar concentrations of the leaf extracts. The experiment was done in triplicate.

The following formula was used to calculate the percent (%) inhibition of DPPH (17):-

$$\text{Scavenging effect (\%)} = [(A_0 - A/A_0)] \times 100$$

Where,

A_0 = absorbance of the blank solution (DPPH without extract)

A = absorbance of the extract + DPPH

2,2'-azinobis-(3-ethylbenzothiazoline-6-sulfonic acid (ABTS)

The 2,2'-azinobis-(3-ethylbenzothiazoline-6-sulfonic acid (ABTS) radical scavenging activity of the leaf extracts of *B. coriacea* and *U. leptocladon* was determined using the method described by Re et al (1999) (18). First ABTS radical was produced by reaction of 7 mM solution of ABTS in water with 2.45 mM potassium persulphate ($K_2O_8S_2$) (1:1). The mixture was held in darkness at 27°C for 16 h. After 16 h, the ABTS radical solution was further diluted with distilled water until the initial absorbance was reached 0.7 at 734 nm. Stock solutions of 1mg/ml of the extract was diluted to different concentrations ranging from 0.025 to 0.2 mg/mL (0.025, 0.05, 0.1, 0.15, and 0.2 mg/mL). Then, 1.9 ml of ABTS working solution was mixed with 0.1 ml of the extract or standard. Ascorbic acid was used as standard. Absorbance was taken at 734 nm using spectrophotometer (UV-UV/Vis/NIR spectrophotometer, Perkin Elemer, Lambda 950). The experiment was done in triplicates.

The following formula was used to calculate the percent (%) inhibition of ABTS (18):-

$$\% \text{ ABTS inhibition} = \frac{[(A_{\text{blank}} - A_{\text{sample}})] \times 100}{A_{\text{blank}}}$$

Where,

A_{blank} = the absorbance of the blank solution (ABTS without the extract)

A_{sample} = the absorbance of the extract + ABTS

Ferric Reducing Antioxidant Power (FRAP) assay

The ferric reducing antioxidant power of the leaf extracts of *B. coriacea* and *U. leptocladon* was determined using the method described by Benzie and Strain (1996) (19). First, stock solutions of 300 mM acetate buffer, 10 mM TPTZ (2, 4, 6-tripyridyl-s-triazine) solution in 40 mM HCl, and 20 mM $FeCl_3 \cdot 6H_2O$ solution were prepared. Then, fresh FRAP solu-

tion was prepared by mixing 25 ml acetate buffer, 2.5 ml TPTZ, and 2.5 mL $FeCl_3 \cdot 6H_2O$. Then, the FRAP solution was incubated at 37°C for 30 min. After 30 min of incubation at 37°C, 100 μ L of the plant extract (0.1 mg/mL) was allowed to react with 2900 μ L of the FRAP solution for 30 min in the dark. Finally, absorbance was read at 593 nm using spectrophotometer (UV-UV/Vis/NIR spectrophotometer, Perkin Elemer, Lambda 950). Ferrous sulfate ($FeSO_4$) was used as standard (different concentrations ranging from 10 to 80 μ g/mL). The experiment was performed in triplicates. Results are expressed in μ M Fe (II)/g dry mass. The following formula was used to calculate the FRAP of the crude extracts and fractions of the leaf extracts of *B. coriacea* and *U. leptocladon* (20):-

$$\text{FRAP value } (\mu\text{M Fe (II)/g dry mass}) = c \times V \times t/m$$

Where, FRAP value (c) is the $FeSO_4$ concentration (μ mol/mL) calculated from the $FeSO_4$ calibration curve, V is the extract volume (mL), t is the dilution factor, and m is the mass of the extract (g).

Determination of total phenolic content

Total phenolic content of the leaf extracts of *B. coriacea* and *U. leptocladon* was determined by using the Folin-Ciocalteu method (21). The reaction mixture was prepared by mixing 1.25 mL of 10% Folin-Ciocalteu reagent (diluted with distilled water 1:10 v/v), 1.25 mL of sodium carbonate (7.5%) and 0.25 mL of extract in CH_3OH (0.1 mg/mL). Then, the mixture was incubated for 45 min under dark condition. The absorbance was measured at 760 nm using spectrophotometer (UV-UV/Vis/NIR spectrophotometer, Perkin Elemer, Lambda 950). Gallic acid was used as standard (different concentrations ranging from 20 to 140 μ g/mL). The experiment was done in triplicates. Results were expressed in mg Gallic acid equivalents (GAE) per gram dry extract weight. The following formula was used to calculate the total phenol content in the crude extracts and fractions of the leaf extracts of *B. coriacea* and *U. leptocladon* (21):-

$$C = c \cdot V / m$$

Where, C = total phenolic content mg GAE/g dry extract, c = concentration of Gallic acid calculated from the Gallic acid calibration curve in mg/mL, V = volume of extract (mL), and m = mass of extract (g).

Determination of total flavonoid content

Total flavonoid content in the leaf extracts of *B. coriacea* and *U. leptocladon* was determined by using aluminum chloride colorimetric assay (22). Sodium nitrate (0.15 mL of 5 %) was added to 0.25 ml extract in CH_3OH (0.1 mg/mL). After 5 min,

0.15 mL of 10 % AlCl₃ was added and left for 5 min. Then, 1 mL of 1 M NaOH was added into the solution and filled with CH₃OH to make final volume to 5 mL. Finally, the solutions were allowed to stand for 30 minutes in the dark at room temperature. Absorbance of the mixture was measured at 510 nm using spectrophotometer (UV-UV/Vis/NIR spectrophotometer, Perkin Elemer, Lambda 950). Quercetin was used as standard (different concentrations in MeOH ranging from 25 to 150 µg/mL). The experiment was performed in triplicates. Total flavonoid content was expressed in mg quercetin equivalent (QE) per gram dry extract weight (mg/g). The following formula was used to calculate the total flavonoid content in the crude extracts and fractions of the leaf extracts of *B. coriacea* and *U. leptocladon* (22):-

$$C=c.V/m$$

Where, C=total flavonoid content mg QE/g dry extract, c=concentration of quercetin calculated from the quercetin calibration curve (mg/mL), V=volume of extract (mL), and m=mass of extract (g).

Data analysis

The DPPH and ABTS radical scavenging activities of the leaf extracts of *B. coriacea* Graells and *U. leptocladon* Oliv were expressed as IC₅₀ and mean percent inhibition ± SD (mean ± SD). The FRAP of the leaf extracts was expressed as µM Fe (II)/g dry extract (mean ± SD). Total phenol content was ex-

pressed as mg Gallic acid equivalent per gram of dry extract (mean ± SD). Total flavonoid content was expressed as mg quercetin equivalent per gram of dry extract (mean ± SD). P<0.05 was considered statistically significant. Analysis of the difference between the antioxidant activities of the different groups was performed using one-way analysis of variance (ANOVA) with post hoc comparison (Tukey's test).

Ethical consideration

Ethical clearance (IRB/03/14/2022) was obtained from the Institutional Review Board (IRB) of the College of Natural and Computational Sciences, Addis Ababa University.

Result

DPPH radical scavenging activity of the leaf extract of *B. coriacea*

The different concentrations of *B. coriacea* (the crude extract and fractions of *B. coriacea*) had dose dependent DPPH antioxidant activities. The CH₃OH:CHCl₃ fraction of *B. coriacea* leaf extract (IC₅₀=38.2 µg/mL) demonstrated the highest DPPH radical scavenging activity as compared with the other three fractions of *B. coriacea* leaf extract (CHCl₃, CH₃OH, and Petroleum ether fractions) (Table 1). The Petroleum ether fraction of *B. coriacea* showed the lowest DPPH radical scavenging activity (IC₅₀=1149 µg/mL).

Table 1: DPPH free radical scavenging activity by the crude extract and fractions of the leaf extract of *B. coriacea*

Concentrations (µg/mL)	Percent inhibition of DPPH (%) (mean±SEM)						
	Crude extract of <i>B. coriacea</i>	CH ₃ OH: CHCl ₃ fraction of <i>B. coriacea</i>	CHCl ₃ of	CH ₃ OH fraction of <i>B. coriacea</i>	CHCl ₃ fraction of <i>B. coriacea</i>	Petroleum ether fraction of <i>B. coriacea</i>	Ascorbic acid
20	38±0.63 bcdef*	47±0.005 acdef*		23±0.22 abdef*	21±0.01 abcef*	16±0.01 abcdf*	45±0.005 abcde*
40	45±0.37 bcdef*	51±0.04 acdef*		25±0.01 abdef*	23±0.16 abcef*	17±0.05 abcdf*	55±0.003 abcde*
80	52±0.61 bcdef*	55 ±0.04 acdef*		27±0.72 abdef*	25±0.01 abcef*	18 ±0.05 abcdf*	65±0.01 abcde*
120	58±0.021 bcdef*	60±0.006 acdef*		30±0.01 abdef*	27±0.03 abcef*	20 ±0.05 abcdf*	75±0.02 abcde*
160	65±0.6 cdef*	65±0.005 cdef*		32±0.01 abdef*	29±0.14 abcef*	21 ±0.05 abcd*	85 ± 0.02 abcde*
200	71.4±0.63 bcdef*	69±0.01 acdef*		34±0.02 abdef*	31±0.03 abcef*	22 ±0.6 abcd*	98.9±0.02 abcde*
IC ₅₀ (µg/mL)	74.2 bcdef*	38.2 acdef*		462 abdef*	590 abcef*	1149 abcdf*	30.5 abcde*

Note: SEM stands for standard error of the mean. * indicates the mean difference is significant at p<0.05. a: compared with crude extract of *B. coriacea*, b: compared with CH₃OH: CHCl₃ fraction, c: compared with CH₃OH fraction, d: compared with CHCl₃ fraction, e: compared with Petroleum ether fraction, f: compared with ascorbic acid.

DPPH radical scavenging activity of the leaf extract of *U. leptocladon*

The different concentrations of *U. leptocladon* (the crude extract and fractions of *U. leptocladon*) had dose dependent DPPH antioxidant activities. The C₂H₆OH fraction of *U. leptocladon* leaf extract (IC₅₀=30.5 µg/mL) demonstrated the

highest DPPH radical scavenging activity as compared with the other two fractions of *U. leptocladon* leaf extract (CHCl₃ and C₄H₈O₂ fractions) (Table 2). The C₄H₈O₂ fraction of *U. leptocladon* showed the lowest DPPH radical scavenging activity (IC₅₀=1175 µg/mL).

Table 2: DPPH free radical scavenging activity by the crude extract and fractions of the leaf extract of *U. leptocladon*

Concentrations (µg/mL)	Percent inhibition of DPPH (%) (mean±SEM)				
	Crude extract of <i>U. leptocladon</i>	CHCl ₃ fraction of <i>U. leptocladon</i>	C ₄ H ₈ O ₂ fraction of <i>U. leptocladon</i>	C ₂ H ₆ OH fraction of <i>U. leptocladon</i>	Ascorbic acid
20	45±0.01 bcd*	23 ±0.02 acde*	15±0.24 abde*	48±0.01 abce*	45± 0.005 bcd*
40	53±0.04 bcde*	27 ±0.02 acde*	16±0 abde*	52±0.02 abce*	55±0.003 abcd*
80	63±0.01 bcde*	32 ±0.005 acde*	17±0.006 abde*	56±0.03 abce*	65±0.01 abcd*
120	71±0.08 bcde*	36±0.01 acde*	18±0.03 abde*	60±0.11 abce*	75±0.02 abcd*
160	80±0.01 bcde*	41 ±0.02 acde*	19±0.005 abde*	65±0.008 abce*	85 ±0.02 abcd*
200	91±0.005 bcde*	46 ±0.02 acde*	20±0.04 abde*	69±0.39 abce*	98.9±0.02 abcd*
IC₅₀ (µg/mL)	33.5 bcde*	238 acde*	1175 abde*	30.5 abc*	30.5 abc*

Note: SEM stands for standard error of the mean. * indicates the mean difference is significant at p<0.05. a: compared with crude extract of *U. leptocladon*. b: CHCl₃ fraction, c: compared with C₄H₈O₂ fraction, d: compared with C₂H₆OH fraction, e: compared with ascorbic acid.

DPPH radical scavenging activity of Isolated compounds

The antioxidant activity of the compounds isolated from leaf extracts of *B. coriacea* and *U. leptocladon* was shown in Table 3. The antioxidant effects of the leaf extract of *B. coriacea* is due to β-sitosterol and lucidine-type compound. The antioxidant effects of the leaf extract of *U. leptocladon* is attributed to β-sitosterol, β-sitosterol glucoside, and α-humulene. The highest DPPH antioxidant activity was shown by the lucidine type compound (IC₅₀=48.5 µg/mL). 1-tricontanol demonstrated the lowest antioxidant activity (IC₅₀=572.2 µg/mL).

ABTS radical scavenging activity

ABTS radical scavenging activity by the leaf extract of *B. coriacea*

Table 4 shows ABTS radical scavenging activity of the crude extract and fractions of the leaf extract of *B. coriacea*. The

findings revealed that the different concentrations of *B. coriacea* (the crude extract and fractions of *B. coriacea*) had dose dependent ABTS antioxidant activity.

The CH₃OH: CHCl₃ fraction of *B. coriacea* leaf extract (IC₅₀=70 µg/mL) demonstrated the highest ABTS radical scavenging activity as compared with the other three fractions of *B. coriacea* (CHCl₃, CH₃OH, and Petroleum ether fractions) (Table 4). The Petroleum ether fraction of *B. coriacea* showed the lowest ABTS radical scavenging activity (IC₅₀=382.6 µg/mL).

Table 3: Antioxidant activity by the compounds isolated from leaf extracts of *B. coriacea* and *U. leptocladon* using DPPH radical scavenging assay

Concentrations ($\mu\text{g/mL}$)	Percent inhibition of DPPH (%) (mean \pm SEM)					
	β -sitosterol	β -sitosterol glucoside	α -humulene	Lucidine type compound	1-tricontanol	Ascorbic acid
20	26 \pm 0.06 bcdef*	30 \pm 0.03 acdef*	23 \pm 0 abdef*	40 \pm 0.005 abcef*	5 \pm 0.17 abcdf*	45 \pm 0.008 abcde*
40	31 \pm 0.01 bcdef*	35 \pm 0.01 acdef*	28 \pm 0.08 abdef*	48 \pm 0.003 abcef*	8 \pm 0.003 abcdf*	55 \pm 0.008 abcde*
80	41 \pm 0.005 bcdef*	50 \pm 0.05 acdef*	38 \pm 0.003 abdef*	61 \pm 0.33 abcef*	11 \pm 0.02 abcdf*	65.7 \pm 0.005 abcde*
120	55 \pm 0.05 bcdef*	65 \pm 0.003 acdef*	53 \pm 0.008 abdef*	72 \pm 0.006 abcef*	14 \pm 0.003 abcdf*	76.8 \pm 0.008 abcde*
160	70 \pm 0.005 bcdef*	80 \pm 0.01 acdef*	68 \pm 0.01 abdef*	85 \pm 0.003 abcef*	17 \pm 0.003 abcdf*	90 \pm 0.006 abcde*
200	85 \pm 0.01 bcdef*	95 \pm 0.003 acdef*	83 \pm 0.006 abdef*	96.7 \pm 0.008 abcef*	20 \pm 0.01 abcdf*	98.6 \pm 0.005 abcde*
IC ₅₀ ($\mu\text{g/mL}$)	99 bcdef*	77.6 acdef*	105.6 abdef*	48.5 abcef*	572.2 abcdf*	29.3 abcde*

Note: a: compared with β -sitosterol, b: compared with β -sitosterol glucoside; c: compared with α -Humulene; d: compared with lucidine type compound; e: compared with 1-tricontanol; f: compared with ascorbic acid. SEM stands for standard error of the mean. * indicates the mean difference is significant at $p < 0.05$.

Table 4: ABTS radical scavenging activity by crude extract and fractions of the leaf extract of *B. coriacea*

Concentration ($\mu\text{g/mL}$)	Percent ABTS inhibition (mean \pm SEM)					
	Crude extract of <i>B. coriacea</i>	CH ₃ OH: CHCl ₃ fraction of <i>B. coriacea</i>	CH ₃ OH fraction of <i>B. coriacea</i>	CHCl ₃ fraction of <i>B. coriacea</i>	Petroleum ether fraction of <i>B. coriacea</i>	Ascorbic acid
25	38 \pm 0.03 bcdef*	40 \pm 0.05 acdef*	34 \pm 0.01 abdef*	22 \pm 0.02 abcef*	21 \pm 0.02 abcdf*	49 \pm 0.03 abcde*
50	45 \pm 0.03 bcdef*	46 \pm 0.08 acdef*	41 \pm 0.01 abdef*	25 \pm 0.01 abcef*	24 \pm 0.04 abcdf*	58 \pm 0.01 abcde*
100	56 \pm 0.03 cdef*	56 \pm 0.02 cdef*	49 \pm 0.01 abdef*	29 \pm 0.006 abcef*	28 \pm 0.01 abcdf*	72 \pm 0.02 abcde*
150	68 \pm 0.03 bcdef*	66 \pm 0.02 acdef*	57 \pm 0.01 abdef*	33 \pm 0.03 abcef*	32 \pm 0.01 abcdf*	89 \pm 0.3 abcde*
200	81.3 \pm 0.05 bcdef*	76.7 \pm 0.02 acdef*	66 \pm 0.05 abdef*	37 \pm 0.01 abcef*	36 \pm 0.01 abcdf*	99 \pm 0.08 abcde*
IC ₅₀ ($\mu\text{g/mL}$)	74 bcdef*	70 acdef*	106.2 abdef*	370 abcef*	382.6 abcdf*	24 abcde*

Note: SEM stands for standard error of the mean. * indicates the mean difference is significant at $p < 0.05$. a: compared with crude extract of *B. coriacea*, b: compared with CH₃OH: CHCl₃ fraction, c: compared with CH₃OH fraction, d: compared with CHCl₃ fraction, e: compared with Petroleum ether fraction, f: compared with ascorbic acid.

ABTS radical scavenging activity the leaf extract of *U. leptocladon*

Both the crude extract and fractions of the leaf extract of *U. leptocladon* showed ABTS radical scavenging activity (Table 5). The findings revealed that the different concentrations of *U. leptocladon* (the crude extract and fractions of *U. leptocladon*) had dose dependent ABTS antioxidant activities.

The C₂H₆OH fraction of *U. leptocladon* leaf extract (IC₅₀=24.4 $\mu\text{g/mL}$) demonstrated the highest ABTS radical scavenging activity as compared with the other two fractions (CHCl₃ and C₄H₈O₂ fractions) (Table 5). The C₄H₈O₂ fraction of *U. leptocladon* showed the lowest ABTS radical scavenging activity (IC₅₀=658.6 $\mu\text{g/mL}$).

Table 5: ABTS radical scavenging activity by crude extract and fractions of the leaf extract of *U. leptocladon*

Concentrations ($\mu\text{g/mL}$)	Percent inhibition of ABTS (%) (mean \pm SEM)				
	Crude extract of <i>U. leptocladon</i>	CHCl_3 fraction of <i>U. leptocladon</i>	$\text{C}_4\text{H}_8\text{O}_2$ fraction of <i>U. leptocladon</i>	$\text{C}_2\text{H}_6\text{OH}$ fraction of <i>U. leptocladon</i>	Ascorbic acid
25	49 \pm 0.01 bcd*	41 \pm 0.02 acde*	18 \pm 0.02 abde*	48 \pm 0.03 abce*	49 \pm 0.03 bcd*
50	57 \pm 0.03 bcde*	51 \pm 0.006 acde*	20 \pm 0.01 abde*	58 \pm 0.01 abc*	58 \pm 0.01 abc*
100	71 \pm 0.3 bcde*	61 \pm 0.01 acde*	22 \pm 0.6 abde*	68 \pm 0.005 abce*	72 \pm 0.02 abcd*
150	87 \pm 0.04 bcde*	71 \pm 0.02 acde*	25 \pm 0.03 abde*	78 \pm 0.05 abce*	89 \pm 0.3 Abcd*
200	96 \pm 0.04 bcde*	83 \pm 0.03 acde*	27 \pm 0.01 abde*	90 \pm 0.14 abce*	99 \pm 0.08 abcd*
IC₅₀ ($\mu\text{g/mL}$)	25.2 Bcde	54.9 acde*	658.6 abde*	24.4 abc*	24 abc*

Note: SEM stands for standard error of the mean. * indicates the mean difference is significant at $p < 0.05$. a: compared with crude extract of *U. leptocladon*. b: CHCl_3 fraction, c: compared with $\text{C}_4\text{H}_8\text{O}_2$ fraction, d: compared with $\text{C}_2\text{H}_6\text{OH}$ fraction, e: compared with ascorbic acid.

FRAP of the leaf extracts of *B. coriacea* and *U. leptocladon*

The FRAP of the leaf extracts of *B. coriacea* and *U. leptocladon* was calculated based on the standard curve of FeSO_4 . The ability of the crude leaf extracts of *B. coriacea* and *U. leptocladon* to reduce TPRZ-Fe (III) complex to TPTZ-Fe (II) were found to be $887.6 \pm 0.41 \mu\text{M Fe(II)/g dry mass}$ and

$1680 \pm 0.13 \mu\text{M Fe(II)/g dry mass}$, respectively. The MeOH:CHCl_3 fraction of *B. coriacea* ($940.1 \pm 2.87 \mu\text{M Fe(II)/g dry mass}$) and the $\text{C}_2\text{H}_6\text{OH}$ fraction of *U. leptocladon* ($1842.6 \pm 0.85 \mu\text{M Fe(II)/g dry mass}$) had the highest ferric reducing potential (Table 6).

Table 6: FRAP of the leaf extract of *B. coriacea* and *U. leptocladon*

Plant name	Plant extract/fractions	$\mu\text{M Fe(II)/g dry mass}$ (mean \pm SEM)
<i>B. coriacea</i>	Crude extract	815.3 \pm 0.24 bcdefghi*
	$\text{CH}_3\text{OH:CHCl}_3$ fraction	940.1 \pm 1.65 acdefghi*
	CH_3OH fraction	389.4 \pm 0.04 abdefgh*
	CHCl_3 fraction	374.9 \pm 0.04 abcdefghi*
	Petroleum ether fraction	374.8 \pm 0.04 abcdefghi*
<i>U. leptocladon</i>	Crude extract	1680 \pm 0.07 abcdefghi*
	$\text{C}_2\text{H}_6\text{OH}$ fraction	1842.6 \pm 0.07 abcdefghi*
	CHCl_3 fraction	809.6 \pm 0.05 abcdefghi*
	$\text{C}_4\text{H}_8\text{O}_2$ fraction	388.8 \pm 0.04 abdefgh*

Note: a: compared with crude extract of *B. coriacea*; b: compared with $\text{CH}_3\text{OH:CHCl}_3$ fraction of *B. coriacea*; c: CH_3OH fraction of *B. coriacea*; d: CHCl_3 fraction of *B. coriacea*; e: Petroleum ether fraction of *B. coriacea*; f: crude extract of *U. leptocladon*; g: $\text{C}_2\text{H}_6\text{OH}$ fraction of *U. leptocladon*; h: CHCl_3 fraction of *U. leptocladon*; i: $\text{C}_4\text{H}_8\text{O}_2$ fraction of *U. leptocladon*. * indicates the mean difference is significant at $p < 0.05$. SEM stands for standard error of mean.

Determination of total phenol and flavonoid content

The crude extract of *B. coriacea* and *U leptocladon* had total phenol contents of 137.7 and 147.7 mg/g of dry extract, respectively (Table 7). The highest total phenol content was obtained in the CH₃OH: CHCl₃ (145.00 mg/g of dry extract) and C₂H₆OH (187.70 mg/g of dry extract) fractions in the *B. coriacea* and *U leptocladon*, respectively. Meanwhile the least concentrations of total phenol were found in the petroleum ether (11.60 mg/g of dry extract) and C₄H₈O₂ (10.90 mg/g of dry extract) fractions, respectively.

The total flavonoid content was highest in the crude extracts of both *B. coriacea* (111.70 mg/g of dry extract) and *U. leptocladon* (138.80 mg/g of dry extract). Among the fractions, the highest total flavonoid content was obtained in the CH₃OH:CHCl₃ (136.80 mg/g of dry extract) and C₂H₆OH (172.90 mg/g of dry extract) fractions in the *B. coriacea* and *U leptocladon*, respectively. In contrast, the least concentrations were found in the petroleum ether (0.75 mg/g of dry extract) and C₄H₈O₂ (4.24 mg/g of dry extract) fractions, respectively (Table 7).

Table 7: Total phenolic and total flavonoid content of the leaf extracts of *B. coriacea* and of *U. leptocladon*

Plant name	Test sample	Total phenolic content (mg /g dry extract) (mean ± SEM)	Total flavonoid content (mg/g dry extract) (mean ± SEM)
<i>B. coriacea</i>	Crude extract	137.7± 0.34 bcdefghi*	111.7±0.051 bcdefghi*
	CH ₃ OH: CHCl ₃ fraction	145± 0.01 acdefghi*	136.8±0.03 acdefghi*
	CH ₃ OH fraction	24.8± 0.01 abdefghi*	9.75±0.01 abdefghi*
	CHCl ₃ fraction	12.3±0.01 abcdefghi*	3.8±0.03 abcdefgh*
	Petroleum ether fraction	11.6± 0.03 abcdefgh*	0.75±0.005 abcdefghi*
<i>U. leptocladon</i>	Crude extract	147.7± 0.01 abcdefghi*	138.8± 0.05 abcdefghi*
	C ₂ H ₆ OH fraction	187.7±0.03 abcdefghi*	172.9±0.23 abcdefghi*
	CHCl ₃ fraction	41.3±0.06 abcdefghi*	22.05±0.03 abcdefghi*
	C ₄ H ₈ O ₂ fraction	10.9 ±0.005 abcdefgh*	4.24 ± 0.15 abcdefgh*

Note: a: compared with crude extract of *B. coriacea*; b: compared with CH₃OH: CHCl₃ fraction of *B. coriacea*; c: CH₃OH fraction of *B. coriacea*; d: CHCl₃ fraction of *B. coriacea*; e: Petroleum ether fraction of *B. coriacea*; f: crude extract of *U. leptocladon*; g: C₂H₆OH fraction of *U. leptocladon*; h: CHCl₃ fraction of *U. leptocladon*; i: C₄H₈O₂ fraction of *U. leptocladon*. * indicates the mean difference is significant at p<0.05. SEM stands for standard error of mean.

Discussion

This study showed that the leaf extracts of *B. coriacea* and *U. leptocladon* have potent DPPH and ABTS radicals scavenging effects. Based on the IC₅₀ value, the ability of DPPH radical scavenging activity of antioxidants can be classified in to five groups:- highly active (IC₅₀ < 50 µg/mL); active (IC₅₀ 50-100 µg/mL); moderate (IC₅₀ 101-250 µg/mL); weak (IC₅₀ 250 to 500 µg/mL) and inactive (IC₅₀ >500 µg/mL) (23). Accordingly, the crude extract of *U. leptocladon* (IC₅₀=33.5 µg/mL), the CH₃OH:CHCl₃ fraction of *B. coriacea* (IC₅₀=38.2 µg/mL), the C₂H₆OH fraction of *U. leptocladon* (IC₅₀=30.5 µg/mL) and the lucidine type compound (IC₅₀=48.5 µg/mL) are highly active in their DPPH radical

scavenging activity. Whereas, β-sitosterol glucoside (IC₅₀=77.6 µg/mL) and the crude extract of *B. coriacea* (IC₅₀=74.2 µg/mL) demonstrated to be active against the DPPH radical. β-sitosterol (IC₅₀=99 µg/mL) and α-humulene (IC₅₀=105.6 µg/mL) had moderate DPPH scavenging activity. In contrast to the other compounds, 1-Tricontanol was inactive against DPPH radical (IC₅₀=572.25 µg/mL). The results of this study substantiate previous studies that investigated the antioxidant activities of the leaf extracts of other *Boscia* species such as *B. senegalensis* and *B. Arabica* (6, 8) and *Uvaria* species such as *U. chamae* (14).

Free radicals scavenging activity of plants is mainly related with their total phenol content (24). Therefore, the high inhibition of ABTS and DPPH by the leaf extract of *B. coriacea* and *U. leptocladon* noted in this study could be due the high

total phenol and flavonoid contents of the plants. Similarly, the highest inhibition of ABTS and DPPH by the CH₃OH:CHCl₃ fraction of *B. coriacea* and the C₂H₆OH fraction of *U. leptocladon* could be due the highest total phenol and flavonoid contents.

Antioxidant activity of medicinal plants is associated with steroids, alkaloids, phenols, flavonoids, and tannins that they possess (25-27). Therefore, the antioxidant activities of the crude leaf extracts of *B. coriacea* Graells and *U. leptocladon* Oliv observed in this study might be due to the presence of alkaloids, phenols, flavonoids, and tannins in the leaf extracts (9).

The ability of FRAP of antioxidants can be classified into five groups as follows (28):- a) Very low: with FRAP value <10 µmol/g; (b) Low: with FRAP value from 10 to 50 µmol/g; (c) Good: with FRAP value from 50 to 100 µmol/g; (d) High: with FRAP value from 100 to 400 µmol/g; Very high: with FRAP value >400 µmol/g. Accordingly, the crude extract of *B. coriacea* (FRAP value=887.6 µmol/g); the crude extract of *U. leptocladon* (FRAP value=1735.6 µmol/g); the CH₃OH:CHCl₃ fraction of *B. coriacea* (FRAP value=940.1 µmol/g); the C₂H₆OH (FRAP value=1828.2 µmol/g) and CHCl₃ fractions of *U. leptocladon* (FRAP value= 809.6 µmol/g) have very high FRAP. Taken together, the leaves extracts of the medicinal plants can be source of potent antioxidant drugs.

Conclusion and recommendation

The study demonstrated that the leaf extracts of *B. coriacea* and *U. leptocladon* have strong antioxidant activity. Further study is needed to determine the mechanism of action of the compounds isolated from the leaves extracts of *B. coriacea* and *U. leptocladon*.

Conflict of interest

There is no conflict of interest in this work.

Reference

1. Rock CL, Jacob RA, Bowen PE. Update of biological characteristics of the antioxidant micronutrients-Vitamin C, Vitamin E and the carotenoids. *J Am Diet Assoc*, 1996; 96:693-702.
2. Taniyama Y, Griendling K.K. Reactive oxygen species in the vasculature. *Hypertension*. 2003; 42:1075–1081.
3. Gilgun-Sherki Y, Rosenbaum Z, Melamed E, Offen D. Antioxidant therapy in acute central nervous system injury: current state. *Pharmacol Rev*. 2002; 54:271–84.
4. Rao AL, Bharani M, Pallavi V. Role of antioxidants and free radicals in health and disease. *Adv Pharmacol Toxicol*. 2006; 7: 29-38.
5. Monon K, Abdoulaye T, Karamoko O, Adama C. Phytochemical composition, antioxidant and antibacterial activities of root of *Uvaria chamae* P. Beauv. (Annonaceae) used in treatment of dysentery in North of Côte d'Ivoire. *Int J Pharmacogn Phytochem Res*. 2015; 7(6): 1047-1053.
6. Vougat R, Foyet H, Garabed R, Ziebe R. Antioxidant activity and phytochemical constituent of two plants used to manage foot and mouth disease in the Far North Region of Cameroon. *J Intercult Ethnopharmacol*. 2015; 4 (1):40-46.
7. Kiswii T, Monda E, Okemo P, Bii C, Alakonya A. Efficacy of selected medicinal plants from Eastern Kenya against *Aspergillus flavus*. *JPS*.2014; 2 (5): 226-231
8. Algfri SK, Qaid AA. Preliminary phytochemical analysis and *in vitro* antioxidant activity of *Boscia arabica* leaves. *Int. J. Pharm. Sci. Rev. Res*. 2021; 68(1): 127-134
9. Tseha ST, Mekonnen Y, Desalegn A, Eyado A, Wondafarsh M. Anti-Inflammatory and Phytochemical Analysis of the Crude Leaves Extracts of *Boscia Coriacea* Graells and *Uvaria Leptocladon* Oliv. *Ethiop J Health Sci*. 2022; 32 (4):817.
10. Okwu DE, Iroabuchi F. Phytochemical composition and biological activities of *Uvaria chamae* and *Clerodendron splendens*. *J Chem*, 2009; 6:553–560.
11. Oluremi BB, Osungunna MO, Omafuma OO. (2010). Comparative assessment of antibacterial activity of *Uvaria chamae* parts. *African J Microbiol Res*. 2010. 4 (13):1391–1394.
12. Bila HA. Phytochemical and antimalarial studies of the leaves of *Uvaria chamae* P.beauv. (Annonaceae). 2016, MSc thesis. Ahmadu Bello University, Zaria-Nigeria.
13. Bamba B, Golly KJ, Ouattara A, Kone M, Doukourou D.N, Benie C.K. et al. Anti-inflammatory activity of the

- aqueous macerate of leaves of *Uvaria chamae* (P. Beauv.) (Annonaceae) on acute edema of Rat paw induced by carrageenan. *IJPPR*. 2019; 11(2):44–8.
14. Nwakaego NL, Chibuike OK, Chukwusgekwu EM, Marylyn AC, Ngozi EI, Chukwunonye ER. *In vitro* antioxidant and free radical scavenging potential of methanolic extracts of *Uvaria Chamae* leaves and roots. *Int J Pharm Pharm Sci*. 2019; 11(1):67-71.
 15. Friis I, Persson E. Flora of Ethiopia and Eritrea. In: Edwards, S., Mesfin, T., Hedberg, I., Sebsebe, D., eds. Volume 2, Part 1. 2000, Addis Ababa University, Addis Ababa, Ethiopia.
 16. Brand-Williams W, Cuvelier M, Berset C. Use of a free radical method to evaluate antioxidant activity. *Lebensm Wiss Technol*, 1995; 28:25-30.
 17. Molyneux P. The use of the stable free radical diphenyl picryldrazyl (DPPH.) for estimating antioxidant activity Song klanakar. *JST*. 2004; 26(2):211-9.
 18. Re R, Pellegrini N, Proteggente A, Pannala A, Yang M, Rice-Evans C. Antioxidant activity: applying an improved ABTS radical cation decolorization assay. *Free Rad Biol Med*. 1999; 26:1231-1237.
 19. Benzie IFF, Strain JJ. The ferric reducing ability of plasma (FRAP) as a measure of antioxidant power: the FRAP assay. *Analyt Bioche*. 1996; 239:70-76.
 20. Xiao F, Xu T, Lu B, Liu R. Guidelines for antioxidant assays for food components. *Food Frontiers*. 2020; 1:60–69.
 21. Singleton V.L, Orthofer, R, Lamuela-Raventos R.M. Analysis of total phenols and other oxidation substrates and antioxidants by means of Folin-CioCalteu reagent. *Methods Enzymol*. 1999; 299: 152-178.
 22. Zhishen J, Mengcheng T, Jianming W. The determination of flavonoid contents in mulberry and their scavenging effects on superoxide radicals. *Food Chem*. 1999; 64:555–9
 23. Jun M, Fu H, Hong J, Wan X, Yang C, Ho C. Comparison of antioxidant activities of isoflavons from Kudzu root (*Pueraria lobata* Ohwi). *J. Food sci*. 2003; 68:2117-2122.
 24. Pourmorad F, Hosseinimehr SJ, Shahabimajd N. Antioxidant activity, phenol and flavonoid contents of some selected Iranian medicinal plants. *African J Biotech*. 2006; 5(11):1142-1145.
 25. Ghosh D. Tannins from Foods to Combat Diseases. *Int J Pharma Res Rev*. 2015; 4(5):40-44.
 26. Iloki-Assanga SB, Lewis-Luján LM, Lara-Espinoza CL, Gil-Salido A, Fernandez-Angulo D., Rubio-Pino J. et al. Solvent effects on phytochemical constituent profiles and antioxidant activities, using four different extraction formulations for analysis of *Bucida buceras* L. and *Phoradendron californicum*. *BMC Res Notes*. 2015; 8:1-14
 27. Fernandes R.P.P, Trindade M.A, Tonin F.G, Lima C.G, Pugine S.M.P, Munekata P.E.S. et al. Evaluation of antioxidant capacity of 13 plant extracts by three different methods: cluster analyses applied for selection of the natural extracts with higher antioxidant capacity to replace synthetic antioxidant in lamb burgers. *J Food Sci Technol*. 2016; 53(1):451–460.
 28. Gan J, Feng Y, He Z, Li X, Zhang H. Correlations between antioxidant activity and alkaloids and phenols of Maca (*Lepidium meyenii*). *J Food Qual*, 2017:1-10.

Anatomic variation of the palmaris longus muscle: A study using the Anatomage Table

Abebe Muche^{1,*} and Abebe Bekele²

¹Department of Human Anatomy, University of Global Health Equity, Kigali, Rwanda, ²Department of Surgery, University of Global Health Equity, Kigali, Rwanda

*Corresponding author: email: abemuche14@gmail.com

Citation: Muche A, Bekele A. Anatomic variation of the Palmaris longus muscle: A study using the Anatomage Table. Ethiop J Health Biomed Sci 2024;14(2):23-30.

DOI: <https://doi.org/10.20372/ejhbs.v14i2.918>

Article History

Received: October 04, 2024

Revised: November 01, 2024

Published: December 31, 2024

Keywords: Palmaris longus muscle, median nerve, anatomical variations, anatomage table, forearm anatomy

Publisher: University of Gondar

Abstract

Background: The palmaris longus muscle, located in the superficial anterior compartment of the forearm, plays a crucial role in wrist flexion.

Objective: This study aimed to investigate the anatomical variation (presence or absence) of the palmaris longus using the Anatomage Table 10.0, a cutting-edge virtual dissection tool.

Method: The research was conducted at the University of Global Health Equity's simulation laboratory in Rwanda from June 10 to June 15, 2024. Five cadavers (2 female, 3 male) with varying resolutions were used to examine the muscle's anatomy. Prior to data collection, instructors received training, and a pilot study ensured the reliability and validity of the research. Virtual dissection and labeling of the palmaris longus muscle and corresponding nerves were performed, while preserving key anatomical structures.

Result: The study revealed a bilateral absence of the palmaris longus muscle in one cadaver.

Conclusion: Our findings on palmaris longus muscle variability highlight the significance of anatomical variations in treatment outcomes and patient care, contributing to the growing understanding of their clinical implications. This variability is crucial for surgeons and clinicians to consider when performing forearm surgeries and diagnosing conditions like carpal tunnel syndrome.

Introduction

The palmaris longus muscle, slender and fusiform in shape, lies within the forearm's superficial anterior compartment. It originates from the common flexor origin near the medial epicondyle, inserts into the palmar aponeurosis, and is innervated by the median nerve. It is positioned between the flexor carpi radialis and flexor carpi ulnaris muscles and partially overlaps the course of the median nerve (1-3).

Like the plantaris muscle, the palmaris longus exhibits considerable morphological variability (4). These variations of the palmaris longus muscle can include complete agenesis, differences in the location and form of the fleshy portion, abnormalities in attachment, duplication or triplication, accessory tendinous slips, and substitutions by elements with similar form or position (5-7).

The variability of the palmaris longus is significant clinically as it can lead to conditions such as compartment syndrome of the forearm and wrist, carpal tunnel syndrome, or Guyon's syndrome. Its anatomic variability can also contribute to diagnostic challenges for radiologists (8, 9). Furthermore, the palmaris longus serves as a key anatomical landmark for surgeries on the forearm and wrist. Its tendon is widely used in reconstructive plastic surgery for tendon grafting and procedures like lip augmentation (10). The palmaris longus also plays a role in ptosis correction (8, 9) and the management of facial paralysis (11).

The Anatomage method revolutionizes human anatomy visualization through its virtual dissection table, providing users with an unprecedented level of accuracy and creating a paradigm shift in anatomy learning. This fully interactive, life-sized touch screen experience mirrors the conditions of working with a fresh cadaver, using genuine patient data at life-like proportions. The Anatomage Table features a life-sized virtual human cadaver displayed on a 2.13×0.67 m screen, offering the ability to digitally dissect the body. By utilizing advanced imaging technologies such as CT scans, X-rays, ultrasound, and MRIs, all integrated into a user-friendly touchscreen interface, the table transforms the study of human anatomy. Users can explore and peel back layers of the digital body, removing structures from the surface to deeper layers. This allows for

the removal of skin to expose muscles, bones, internal organs, nerves, and blood vessels. The table enables students and users to study anatomical structures from multiple perspectives, layers, and scales, promoting a deeper understanding of how the body's parts and organs are interconnected. Anatomage also provides access to anatomical data from both male and female cadavers, sourced from the Visible Human Project (VHP) and the Visible Korean Human (VKH). Additionally, as it is highlighted in studies such as García et al. (2018) ("Possibilities for the use of Anatomage (the anatomical real body-size table) for teaching and learning anatomy with the students") (11).

To our knowledge, this is the first study to analyze palmaris longus muscle variability using the Anatomage Table. The aim of this case study is to enhance understanding of the anatomical differences and variability of the palmaris longus muscle to improve surgical procedures and clinical practices. Based on the Anatomage table study, we found that variations in the presence or absence of the palmaris longus muscle exist among individuals. These variations can significantly impact the planning and execution of surgical procedures involving the forearm and hand, such as carpal tunnel release. The findings underscore the importance of understanding the anatomical differences and variations in the palmaris longus muscle to help surgeons navigate and avoid complications during surgeries in the palmar region.

Material and Method

Study Area and Period

This study was conducted within the simulation laboratory at the University of Global Health Equity in Rwanda. The research took place from June 10 to June 15, 2024, utilizing the Anatomage virtual dissection table 10.0.

Study Design

An observational study design was conducted using an Anatomage virtual dissection Table.

Sample Population

The sample population included all cadavers integrated with the Anatomage Table, consisting of five cadavers (two female and three male). The three cadavers, Hans, Carl and Carla, have a resolution of 0.66mm, 0.66 mm and 1.00 mm while the remaining two, Victor and Vicky have a resolution of 0.80mm in all dimensions (0.80mm, 0.80mm, 0.80mm).

Data Collection

Training and Pilot Study

Before data collection, simulation laboratory instructors underwent two days of training to learn how to use the Anatomage Table and identify anatomical structures such as nerves and muscles. To ensure the reliability and validity of the research instruments, a pilot study was conducted at the University of Global Health Equity. This pilot study focused on the pyramidalis muscle of the abdominal wall, one of the variable muscles, using the Anatomage Table. It involved two cadavers, representing about 30% of the total sample size, and helped identify areas requiring modification.

Data Collection Procedures

The present study utilized Anatomage Table 10.0 to examine variations in the anatomy of the palmaris longus muscle. The latest version, Anatomage Table 10.0, presents meticulously segmented representations of real human anatomy from five cadavers, including a new male cadaver named Hans, reconstructed from a 70-year-old lung cancer patient. Hans pro-

vides unique insights into geriatric anatomy, showcasing detailed muscular and vascular systems (see Fig. 1).

Data collection involved peel of the skin, fascia, and muscles of the thoracic wall and upper limb. Additionally, the skull and lower limb were entirely removed from the cadavers. These virtual dissection procedures were performed using the Anatomage Table's dissection tools. The brachial plexus and its terminal branches, including the ulnar and median nerves, and the bony structures of the upper limb, thoracic wall, and vertebral columns, were preserved intact. Moreover, the palmaris longus muscle, along with its origin and insertion, was left untouched.

Following the isolation of the palmaris longus muscle and corresponding nerves, these structures were labeled using the Pen Tool of the Anatomage Table. The pictures were then saved on the Anatomage Table and exported to a personal computer for further assessment.


Cadavers	Resolution	Sex
Gross Anatomy		
 Victor	0.80 0.80 0.80 (mm)	Male
 Vicky	0.80 0.80 0.80 (mm)	Female
 Hans	0.60 0.60 1.00 (mm)	Male
 Carl	0.66 0.66 1.00 (mm)	Male
 Carla	0.66 0.66 1.00 (mm)	Female

Figure 1: List of cadavers of Anatomage Table with their corresponding resolution and sex (The names are fictional and were randomly assigned by the Anatomage Table company)

Result

Since 2020, the University of Global Health Equity in Rwanda has utilized the Anatomage Table, including its latest version, Anatomage Table 10, across various educa-

tional disciplines such as gross anatomy, histology, physiology, pathology and radiology. During musculoskeletal studies, muscle origins and insertions were extensively explored using the Anatomage Table 10. In a notable discovery during virtual dissection, a bilateral absence of the palmaris longus muscle was observed in one male cadaver named

Carl (Fig. 6). However, in the remaining four cadavers on the Anatomage table, the palmaris longus muscle was clearly distinct in both right and left forearms. Located medial to the median nerve and lateral to the ulnar nerve, the relation-

ship between the palmaris longus and these nerves in the cadavers Victor, Vicky, Hans, and Carla is detailed in Fig. 2, 3, 4, and 5, respectively.

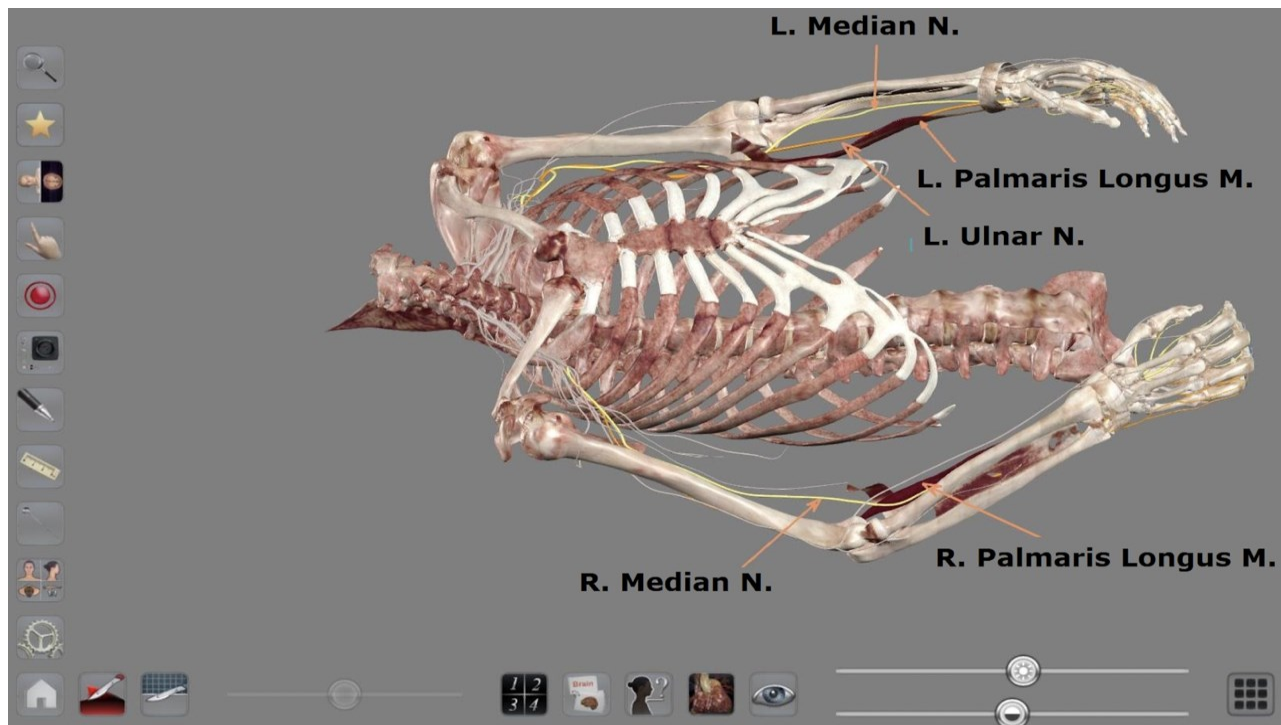


Figure 2: Representation of the relationship between the palmaris longus and the median nerve of a cadaver named Carla. The palmaris longus tendon essentially crosses over the median nerve.

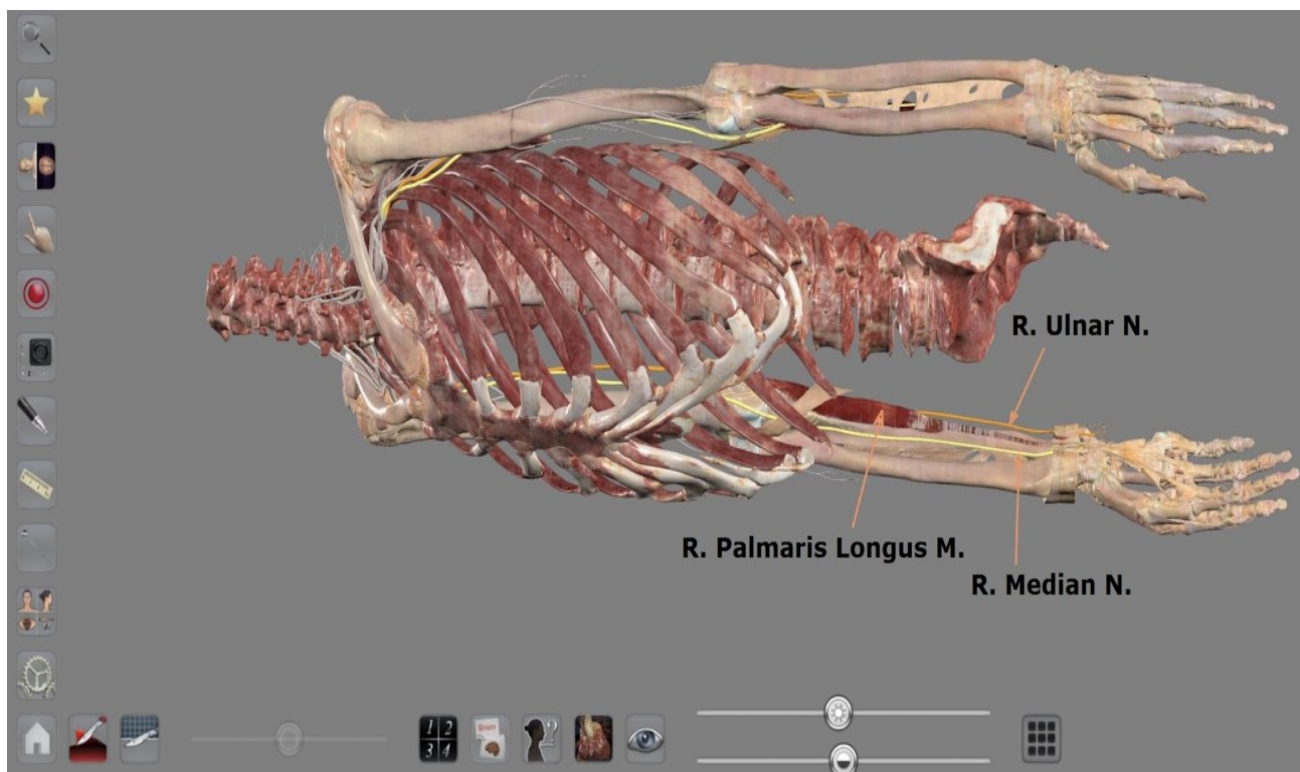


Figure 3: Representation of the relationship between the palmaris longus and the median nerve of a cadaver named Hans. The palmaris longus tendon essentially crosses over the median nerve.

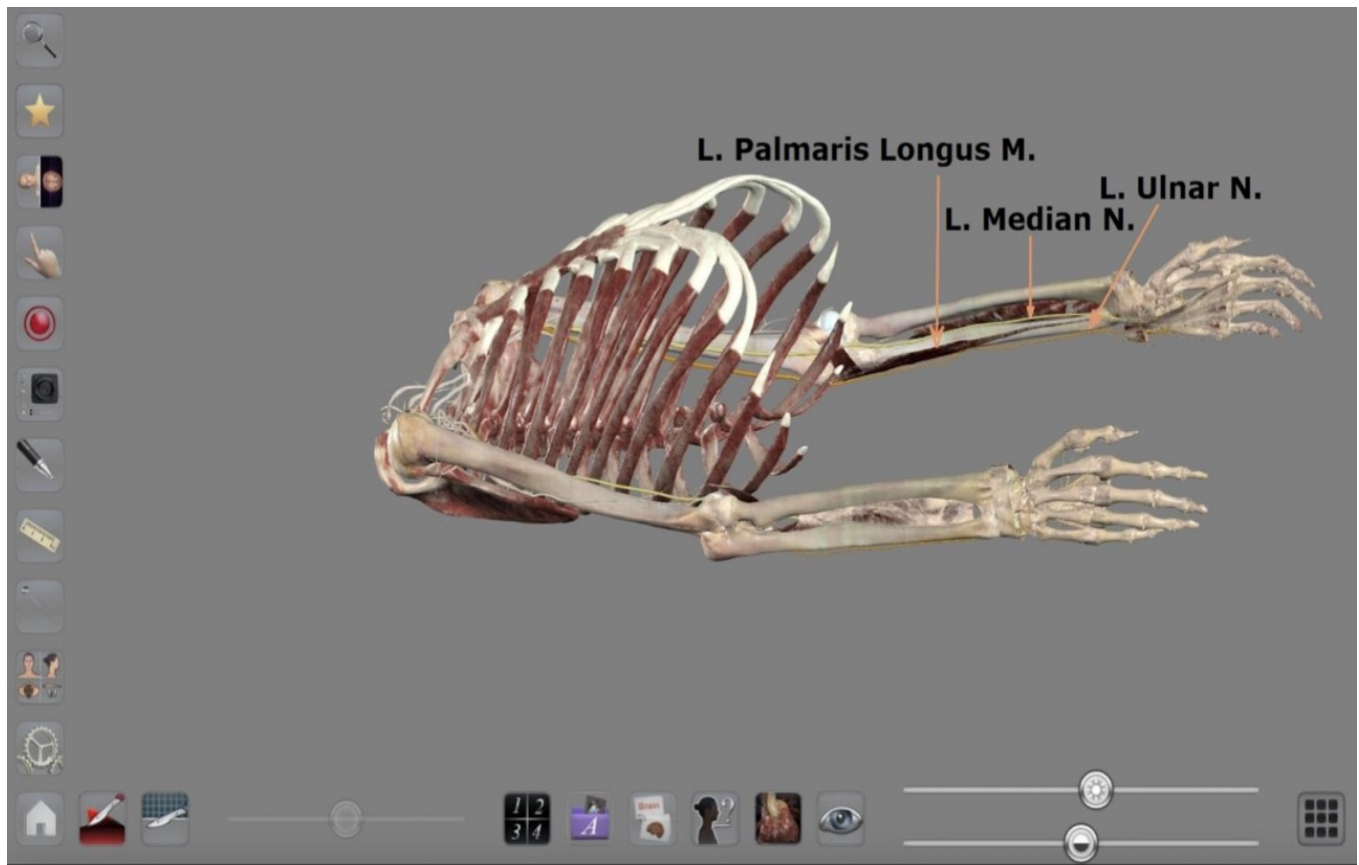


Figure 4: Representation of the relationship between the palmaris longus and the median nerve of a cadaver named Vicky. The palmaris longus tendon essentially crosses over the median nerve.

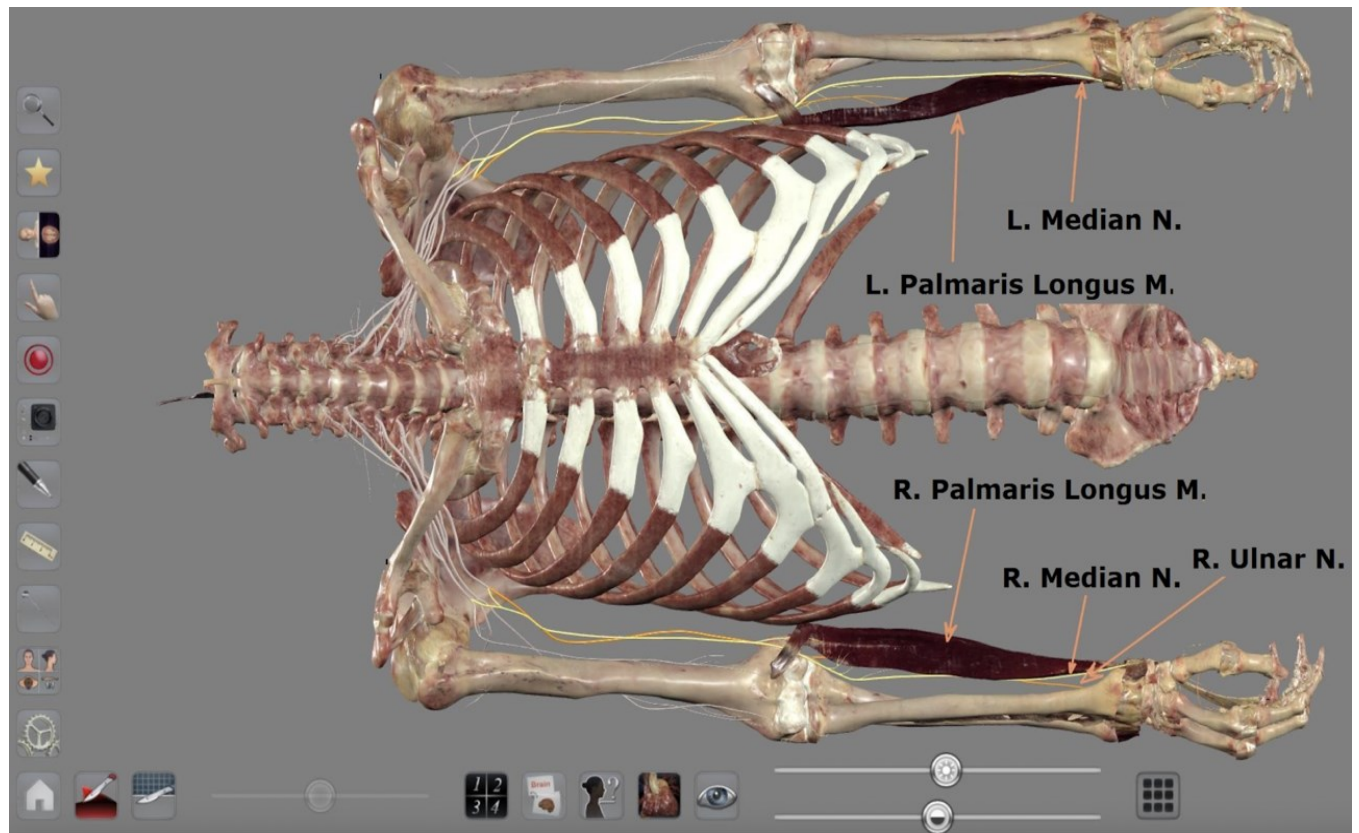


Figure 5: Representation of the relationship between the palmaris longus and the median nerve of a cadaver named Victor. The palmaris longus tendon essentially crosses over the median nerve.

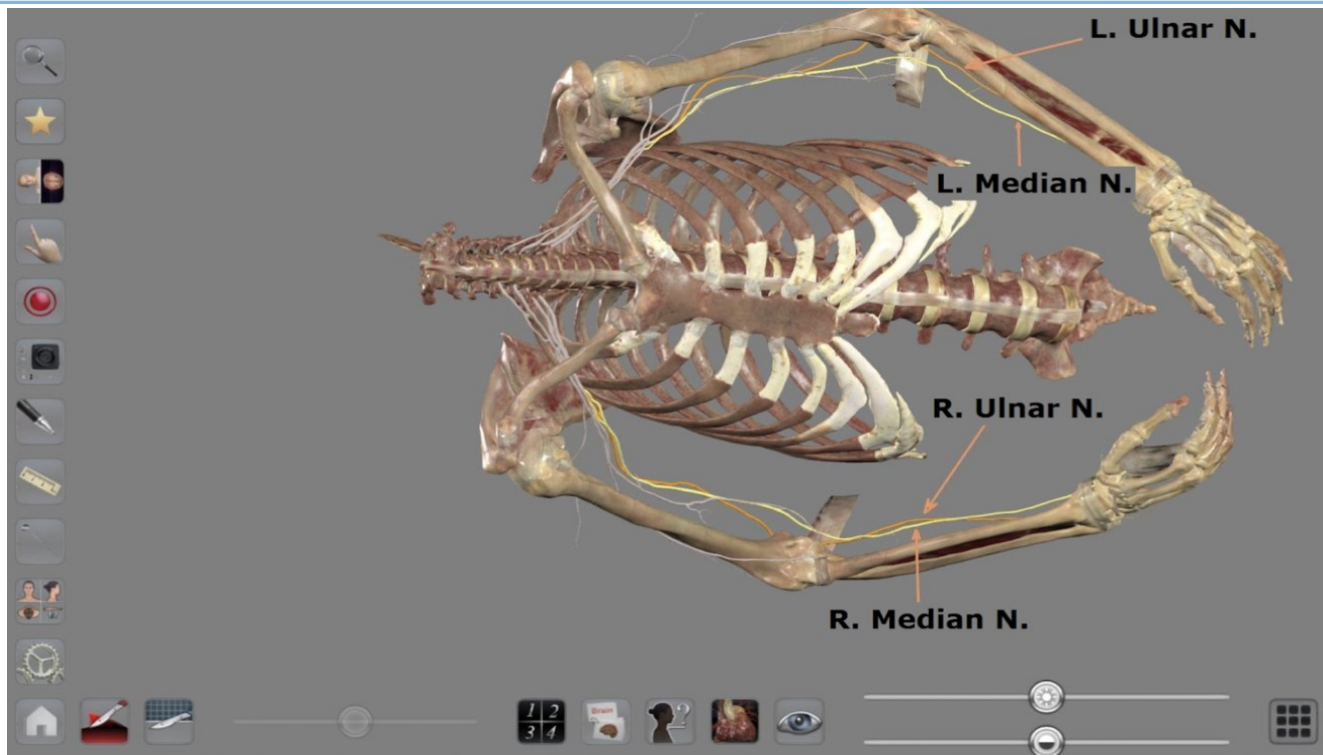


Figure 6: Representation of the bilateral absence of the palmaris longus muscle, highlighting the location of median and ulnar nerve of a cadaver named Carl.

Discussion

A recurring theme in anatomy education is the presence of anatomical variations. During demonstrations, scholars often inquire if these variations are reflected among the cadavers included in the Anatomage table. Our study sheds light on this question by quantifying the proportion of such variations within the palmaris longus muscle. We discovered that 20% of the cadavers (1 of the 5) exhibited a bilateral absence of the palmaris longus muscle.

The palmaris longus, plantaris, pyramidalis, peroneus tertius, and psoas minor muscles are well-recognized for their variability among humans. The palmaris longus, characterized by its short belly and long tendon, has been described as a phylogenetically degenerate metacarpophalangeal joint flexor (14, 15). Found only in mammals, this muscle thrives in species that rely heavily on their forelimbs for movement (16). More specifically, the palmaris longus muscle is well developed in species with a high ratio of upper limb weight to body weight. As this ratio is quite low in humans, the palmaris longus is less developed and its role in the functioning of the hand is reduced. As a result, it may exhibit morphological variation (17). In

humans, the absence of the palmaris longus is possibly dictated by heredity through a mechanism yet to be fully understood (18).

Standard textbooks of surgery estimate a 15% absence rate for the palmaris longus muscle; however, this figure varies considerably across different ethnic groups (19, 20). In the current Anatomage-based study, we found that the palmaris longus muscle was bilaterally absent in one out of five cadavers examined, representing 20% of the cases. A cross-sectional study of 300 Caucasian subjects (150 males and 150 females) aged 18 to 40 years revealed unilateral and bilateral absence rates of 16% and 9%, respectively (21). In contrast, a study of 329 Chinese subjects in Singapore found a unilateral absence rate of 3.3% and a bilateral absence rate of 1.2%, with an overall absence of 4.6% (22).

Moreover, a study conducted in Nigeria reported that about 31.3% of participants lacked the palmaris longus muscle on either side, with 12.5% exhibiting unilateral absence and about 18.8% showing bilateral absence (23). A comparative study in Northern Iran reported an overall prevalence of right-sided, left-sided, bilateral, and total absence of the palmaris longus muscle at 4.1%, 5.2%, 3.9%, and 13.2%, respectively (24).

Our study is limited by the small sample size of cadavers available on the Anatomage Table. While the observed absence is consistent with findings from many other studies, it cannot be deemed statistically significant given the availability of small number of cadavers.

Conclusion

The findings of our Anatomage table study revealed a bilateral absence of the palmaris longus muscle in Caucasian cadaveric specimen. This morphological variability is clinically significant for diagnosing and treating conditions like carpal tunnel syndrome and is relevant for surgical procedures.

Acknowledgment

We are grateful to Dr. Martha Ellen Katz and Ms. Emily Harris from Harvard Medical School for their assistance with language editing. The authors sincerely thank those who donated their bodies to science so that anatomical research could be performed. Results from such research can potentially increase mankind's overall knowledge that can then improve patient care. Therefore, these donors and their families deserve our highest gratitude.

Additional Information

Disclosures

Human subjects: All authors have confirmed that this study did not involve human participants or tissue.

Conflicts of interest:

In compliance with the ICMJE uniform disclosure form, all authors declare the following:

Payment/services info: All authors have declared that no financial support was received from any organization for the submitted work.

Financial relationships: All authors have declared that they have no financial relationships at present or within the previous three years with any organizations that might have an interest in the submitted work.

Other relationships: All authors have declared that there are no other relationships or activities that could appear to have influenced the submitted work.

Reference

1. Ioannis D, Anastasios K, Konstantinos N, Lazaros K, Georgios N. Palmaris Longus Muscle's Prevalence in Different Nations and Interesting Anatomical Variations: Review of the Literature. *J Clin Med Res* 2015;7:825-30.
2. Kumar N, Patil J, Swamy RS, Shetty SD, Abhinitha P, Rao MK, et al. Presence of multiple tendinous insertions of palmaris longus: a unique variation of a retrogressive muscle. *Ethiop J Health Sci.* 2014;24:175-8.
3. Mathew AJ, Sukumaran TT, Joseph S. Versatile but temperamental: a morphological study of palmaris longus in the cadaver. *J Clin Diagn Res* 2015;9(2):AC01-3.
4. Olewnik L, Wysiadecki G, Polguy M, Topol M. Anatomic study suggests that the morphology of the plantaris tendon may be related to Achilles tendonitis. *Surg Radiol Anat* 2017;39:69-75.
5. Natsis K, Levva S, Totlis T, Anastasopoulos N, Paraskevas G. Three-headed reversed palmaris longus muscle and its clinical significance. *Ann Anat.* 2007;189:97-101.
6. Paraskevas G, Tzaveas A, Natsis K, Kitsoulis P, Spyridakis I. Failure of palmaris longus muscle duplication and its clinical application. *Folia Morphol (Warsz).* 2008;67:150-3.
7. Reimann A, Daseler E, Anson B, Beaton L. The Palmaris longus muscle and tendon. A study of 1600 extremities. *Anat Rec.* 1944;89:495-505.
8. Kurihara K, Kojima T, Marumo E. Frontalis suspension for blepharoptosis using palmaris longus tendon. *Ann Plast Surg.* 1984;13:274-8.
9. Naugle TC, Faust DC. Autogeneous palmaris longus tendon as frontalis suspension material for ptosis correction in children. *Am J Ophthalmol.* 1999;127:488-9.
10. Davidson BA. Lip augmentation using the palmaris longus tendon. *Plast Reconstr Surg.* 1995;95:1108-10.
11. Atiyeh BA, Hashim HA, Hamdan AM, Kayle DI, Musharafieh RS. Lower reconstruction and restoration of oral competence with dynamic palmaris longus

- vascularised sling. *Arch Otolaryngol HeadNeck Surg.* 1998;124:1390-2.
12. Raja BS, Chandra A, Azam MQ, Das S, Agarwal A. Anatomage - the virtual dissection tool and its uses: a narrative review. *J Postgrad Med.* 2022, 68:156-61.
 13. Martín JG, Mora CD, Henche SA: Possibilities for the use of anatomage (the Anatomical Real Body-Size Table) for teaching and learning anatomy with the students. *Biomed J Sci Tech Res.* 2018, 4:4080-3.
 14. Koo CC, Roberts AHN. The palmaris longus tendon another variation in its anatomy. *J Hand Surg.* 1997;22-B:138-9.
 15. Gray H, Bennister LH, Berry MM, Williams PL. *Gray's Anatomy: The Anatomical Basis of Medicine and Surgery.* 38 ed. London: Churchill Livingstone /dp/B008ITTNX0; 1999.
 16. Vanderhooft E. The frequency and relationship between the palmaris longus and plantaris tendons. *Am J Orthop.* 1996;25:38-41.
 17. Kumar P. Duplication of palmaris longus muscle. *Int J Anat Var.* 2013;6:207-9.
 18. Wehbe MA, Mawr B. Tendon graft donor sites. *J Hand Surg.* 1992;17-A:1130-2.
 19. Valentine P. Extrinsic muscles of the hand and wrist: An Introduction In: Tubiana R, ed. . *The Hand.* 1. Philadelphia: WB Saunders; 1981. p. 237.
 20. Zancolli EA, Cozzi EP. The retinaculum cutis of the hand. *Atlas of Surgical Anatomy of the Hand.* New York: Churchill Livingstone; 1992. p. 2.
 21. Thompson NW MB, Cran GW. Absence of the palmaris longus muscle: a population study. *Ulster Med J* 2001; 70: 22-4.
 22. Sebastin SJ, Lim AYT, Wong HB. Clinical Assessment of Absence of the Palmaris Longus and its Association With Other Anatomical Anomalies - A Chinese Population Study. *Ann Acad Med Singapore.* 2006;35:249-5.
 23. Kayode AO, Olamide AA, Blessing IO, Victor OU. Incidence of palmaris longus muscle absence in Nigerian population. *Int J Morphol.* 2008;26(2):305-8.
 24. Nasiri E, Pourghasem M, Moladoust H. The Prevalence of Absence of the Palmaris Longus Muscle Tendon in the North of Iran: A Comparative Study. *Iran Red Crescent Med J* 2016 18(3):e22465.

Investigation of Hepatotoxic Effect of Cement-Dust in Occupationally Exposed Individuals in Malete, Kwara State, Nigeria, 2022

Akeem Olayinka Busari^{1*}, Nimotallahi Temitope Omoteji², Idris Yahaya Mohammed³

¹Instituto de Biociências/Faculdade de Ciências Farmacêuticas, Alimentos e Nutrição (INBIO/FACFAN), Universidade Federal de Mato Grosso do Sul, Campo Grande, Brazil, ²Department of Medical Laboratory Science, Kwara State University, Malete, Nigeria, ³Department of Chemical Pathology, Bayero University Kano, Kano State, Nigeria.

*Corresponding Author: Email: busakeem@yahoo.com

Citation: Busari AO, Omoteji NT, Mohammed IY. Investigation of hepatotoxic effect of cement-dust in occupationally exposed individuals at Malete, Kwara State, North Central Nigeria. *Ethiop J Health Biomed Sci* 2024;14(2):31-39.

DOI: <https://doi.org/10.20372/ejhs.v14i2.948>

Article History

Received: November 23, 2024

Revised: December 08, 2024

Published: December 31, 2024

Keywords: Cement dust, hepatotoxic effect, North-Central Nigeria

Publisher: University of Gondar

Abstract

Background: Cement is pivotal in advancing Nigeria's economic and infrastructural development amid rapid urbanization, where the demand for robust infrastructure underscores its integral contribution to meeting developmental requirements. While respiratory concerns have been extensively studied, the impact on the liver with the central role of detoxification remains a critical yet under explored dimension of occupational health.

Objective: Thus, this study investigated the hepatic effect of cement dust exposure among occupationally exposed individuals in North Central Nigeria.

Methods: A comparative cross-sectional study was conducted at Kwara State University Malete, Kwara State, North Central Nigeria, to compare the hepatic profiles of 60 individuals occupationally exposed to cement with 60 non-exposed who served as controls between June and October, 2022. Ethical approval was obtained from the Kwara State Ministry of Health, and informed consent was secured from each participant. Five (5) milliliters of blood were collected, and hepatic profiles were analyzed using standard spectrophotometric methods. Both descriptive and inferential statistics were used to investigate the comparison and correlation between the duration of exposure to cement dust and hepatic profiles among the study participants.

Results: The study revealed a significant increase in alanine aminotransaminase (ALT) and alkaline phosphatase (ALP) activities among individuals exposed to cement (ALT: 30.58 ± 11.54 , ALP: 181.68 ± 26.25) compared to non-exposed controls (ALT: 19.90 ± 7.26 ; ALP: 163.68 ± 29.92) at a significance level of $p < 0.05$. Additionally, the duration of cement dust exposure demonstrated a significant positive correlation with gamma-glutamyl transferase (GGT) activity ($r = 0.363$; $p = 0.004$). Conversely, no significant positive correlation was observed between the duration of cement dust exposure and the activities of aspartate aminotransferase (AST) ($r = 0.190$; $p = 0.147$), ALT ($r = 0.016$; $p = 0.904$), ALP ($r = 0.178$; $p = 0.175$), and direct bilirubin ($r = 0.057$; $p = 0.664$). Furthermore, the duration of cement dust exposure showed a negative and non-significant correlation with total protein ($r = -0.098$; $p = 0.455$), albumin ($r = -0.097$; $p = 0.461$), and total bilirubin ($r = -0.156$; $p = 0.233$).

Conclusion: The study suggests that occupational exposure to cement dust may pose a risk of developing hepatotoxicity in the future.

Copyright: © 2024 at Busari et al. This is an open access article distributed under the terms of the Creative Commons Attribution-NonCommercial 4.0 (CC BY NC 4.0) License, which permits unrestricted use, distribution, and reproduction in any medium, provided the original author and source are credited.

Introduction

Cement dust is mineral dust that contains chemical components such as silicon, calcium, aluminum, chromium, and iron [1]. This dust is formed in several parts of cement manufacturing and processing, including raw material extraction, crushers, rotary kilns, cranes, mills, storage silos, packing areas, and so on. According to Schenker *et al.* [2], cement is a crucial part of concrete that creates the foundation for buildings and roadways, and most of the professionals involved with the use of these materials include tillers, plaster of Paris (POP) installers, construction site workers, and so on. Cement dust contains 60–70% calcium oxide, 17–25% silicon oxide (SiO₂), and 3–5% aluminum oxide, along with iron oxide, chromium, potassium, sodium, sulphur, and magnesium oxide [3].

According to the Occupational Safety and Health Administration, nearly two million workers are exposed to cement dust every day [4]. This dust may enter the human body via the respiratory and gastrointestinal systems, causing harmful effects [5]. Cement dust inclusion particles, diffuse edema, hepatic sinusoidal lining cell proliferation, sarcoid granulomas, and perisinusoidal and portal fibrosis have all been observed in the hepatocytes of cement mill workers. These changes have been linked to liver lesions caused by breathed cement dust [6]. Other organs that might be damaged include the respiratory tract, which is characterized by diseases such as pulmonary embolism, osteo-pulmonary tuberculosis, silicosis, renal diseases, and skin problems that include palm keratinization [7]. The level of toxicity found in short-term exposure may be remedied, but the long-term toxicity is associated with undesirable health consequences [7].

The vast majority of cement workers in Nigeria and other developing nations are unaware of the importance of taking specific precautions to protect their health. Frequently, they are hired without the essential prerequisite training and sent to the job site with or without personal protective equipment [8]. Thus, industrial workers' knowledge and awareness of occupational hazards and how working in excessively dusty conditions affects health and safety is woefully inadequate [9].

A nonchalant attitude towards the use of personal protective devices by cement handlers leads to overly inhalation and

ingestion of cement dust, thereby causing damages such as gastrointestinal and liver damage. Hence, this study evaluated the hepatic profile among cement occupationally exposed individuals to ascertain possible occupational hazards and proper management of already exposed individuals.

Material and Method

Study Area

This study was conducted at Kwara State University (KWASU) Malete, located in Moro Local Government Area of Kwara State, and lies within latitude 8.6563°N to 8.8136°N and longitudes 4.2359°E to 4.5410°E. KWASU has over 30,000 population including undergraduate and graduates students. It is located about 25 km north of Ilorin, the Kwara State capital. Though a relatively virgin area, it is highly vulnerable to unplanned expansions due to its proximity to the state capital and recently the siting of the KWASU campus, which facilitates continuous construction involving cement-occupation exposed individuals both in Malete and KWASU campus. The University provides Health facility accessible to both workers and students and the Medical Laboratory Science Department has standard equipment that aids sample processing, storage, and analysis [10]. The built up area gained an astronomical increase (180%) between 2005 and 2015 while forest lost significantly (34%) within the same periods, with most of the gains occurring in 2010 and 2015 after the establishment of KWASU. The climate of Kwara State exhibits both wet (rainy) and dry seasons in response to the South West Monsoon wind and the North East continental wind which are the major prevailing winds that blow across the state. The wet or rainy season begins towards the end of April and last till October. The dry season begins in November and end in April. The temperature of the state ranges from 33°C to 35°C from November to January and from 34°C to 37°C from February to April. The total annual rainfall ranges from 990.3mm to 1318mm. The rainfall exhibits double maximal pattern. Relative humidity ranges from 75% to 88% from May to October and 35% to 80% during the dry season.

Study Design and period

A comparative cross-sectional study involving cement-exposed workers and unexposed individuals was conducted between June and October, 2022 in KWASU Malete, Kwara State.

The sample size was calculated using the formula for comparative survey

$$n = \frac{(Z_{\alpha/2} + Z_{\beta})^2 \times P1(1-P1) + P2(1-P2)}{(p1 - p2)^2} \quad [11]$$

Where;

P1= proportion of occupational cement exposure in Ekpoma, Nigeria = 4% [12].

P2 = proportion of non-exposed controls

$Z_{\alpha/2}$ = the standard normal deviation (1.96)

Z_{β} = power of the test

n = sample size

$$n = (Z_{\alpha/2} + Z_{\beta})^2 \times P1(1-P1) + P2(1-P2) / (P1-P2)^2$$

The sample size was calculated to be 59 and was increased to 60 to increase the power of the study.

Hence, a total of 120 subjects comprising 60 Cement occupationally exposed individuals and 60 healthy individuals were recruited for this study.

Study Population

The study population includes male and female cement occupationally exposed individuals aged 18 and 50 years and non-exposed age-matched individuals in Malete, Kwara state.

Ethical Approval

Approval for this research was obtained from the Ethical Review Committee of the Kwara State Ministry of Health, Ilorin, with reference number ERC/MOH/2022/05/034 in accordance with the 1975 Helsinki Declaration as revised in 2000. Informed consent was obtained from all participants included in the study.

Inclusion Criteria

Male and female human subjects aged 18–50 years.

Subjects whose duration of exposure to cement is 1 year and above [12].

Exclusion Criteria

Subjects whose exposure duration is less than a year.

Subjects at the extremes of age.

Pregnant women.

Sampling Technique

A convenient random sampling technique was used for the recruitment of study participants, while a detailed questionnaire was provided and given to each participant to fill out.

Data Collection and Sample Analysis

A 5 ml venous fasting blood sample was collected from the superficial vein of the antecubital fossa of each participant and

dispensed into a plain bottle. The sample was allowed to clot and spun at 3000 rpm for 5 minutes to obtain serum. The serum was then separated into another sterile plain tube, which was then used to estimate the serum ALP, serum ALT, serum AST, serum GGT, total protein, bilirubin, and albumin using appropriate methods.

Laboratory Procedure

Serum Albumin Estimation by Dye Binding Method as described by Doumas *et al.* [13].

Principle

In the presence of bromocresol green at a slightly acidic pH, serum albumin produces a color change of the indicator from yellow-green to green-blue. The absorbance of the color produced is measured in a colorimeter at 630 nm, and the intensity of the blue-green color is proportional to the concentration of albumin in the sample.

Quantitative determination of serum total protein by direct biuret method as described by Tietz [14].

Principle

Protein in serum reacts with cupric ions in an alkaline medium to form a blue-colored complex. The intensity of the blue color is proportional to the protein concentration.

Quantitative Estimation of Aspartate Aminotransferase Activities by the Enzymatic Method as Described by Lorentz [15].

Principle

Aspartate aminotransferase catalyzes the reversible transamination of L-aspartate and alpha-ketoglutarate to oxaloacetate and L-glutamate. The oxaloacetate is then reduced to malate in the presence of malate dehydrogenase with the concurrent oxidation of NADH to NAD.

Quantitative Estimation of Serum Alanine Aminotransaminase Activities as Described by Reitman and Frankel [16].

Principle

ALT catalyzes the reversible transfer of an amino group from alanine to alpha-ketoglutarate, forming glutamate and pyruvate. The pyruvate produced is reduced to lactate by lactate dehydrogenase and NADH. The rate of decrease in NADH concentration measured photometrically is proportional to the catalytic concentration of ALT present in the sample.

Quantitative Estimation of Serum Alkaline Phosphatase as Described by King and Armstrong [17].

Principle

ALP catalyzes the hydrolysis of the colorless organic phosphate ester substrate, p-Nitrophenyl phosphate, to the yellow-colored product p-Nitrophenol and phosphate in an alkaline medium of pH 10.3 and the presence of magnesium ions. The increase in the rate of absorbance is proportional to the activity of ALP in the sample.

Quantitative estimation of serum bilirubin as described by Jendrassik and Grof [18].

Principle for Total Bilirubin

Sulfanilic acid reacts with sodium nitrate to form diazotized sulfanilic acid. Total bilirubin reacts with diazotized sulfanilic acid in the presence of TAB to form azobilirubin.

Principle for Direct Bilirubin

Sulfanilic acid reacts with sodium nitrate to form diazotized sulfanilic acid. Direct bilirubin reacts with diazotized sulfanilic acid to form azobilirubin.

Quantitative Estimation of Serum Gamma Glutammy Transferase Activities Using Szasz Methodology [19].

Principle

GGT catalyzes the transfer of a gamma-glutamyl group from the colorless substrate, gamma-glutamyl-p-nitroaniline, to the acceptor glycylglycine with a production of the colored product, p-nitroaniline.

Statistical Analysis

A statistical package for social science (version 20) was used for the statistical analysis. All measured data were presented as mean ± standard deviation. An independent t-test was used to compare the hepatic profile variables between cement-exposed workers and unexposed controls, and the level of significance was considered at P < 0.05.

Result

A total of 60 occupationally exposed and 60 unexposed individuals were recruited for this study (Table 1).The mean age was 27.27 ± 7.38 years, with most participants aged 19-30 (55.3%). Over half were single (67.5%), and the majority identified as Yoruba (73.3%). Half (50%) had a tertiary education with 95% employed full-time. A 50% of the participants had no cement dust exposure, 77.5% never smoked, and 85.8% never consumed alcohol.

Table 1: Socio-Demographic Characteristics of the Study Participants in Maletе, Kwara State, Nigeria, 2022

Variables	Category	Frequency N=120	Percentage (%)
Age (Years)	19-30	67	55.8
	31-40	39	32.5
	41-50	12	10
	51-60	2	1.7
Mean ± SD		27.27±7.38	
Marital Status	Single	81	67.5
	Married	39	32.5
Ethnicity	Yoruba	88	73.4
	Hausa	25	20.8
	Others	7	5.8
Educational Status	Tertiary	60	50
	Secondary	26	21.7
	Primary	25	20.8
	None	9	7.5
Occupation	Students	53	44.2
	Bricklayer	31	25.8
	Cement Loader	19	15.8
	Others	17	14.2
Occupation Options	Full-Time	114	95.0
	Part-Time	6	5.0
Duration of Cement Dust Exposure (Years)	Nil	60	50
	1-4	24	20
	5-10	20	16.7
	11-20	9	7.5
	21-30	7	5.8
Cigarette Smoking	Never	93	77.5
	Daily	11	9.2
	Before	8	6.7
	Others	8	6.6
Alcohol Intake	Never	103	85.8
	Daily	7	5.8
	Others	10	8.3

There was a statistically significant difference when ALT (p=0.000) and ALP (p=0.002) were compared between cement occupationally exposed individuals and healthy non-exposed individuals at p < 0.05. There was no statistically significant difference when AST (p = 0.064), GGT (p = 0.838), total protein (p = 0.213), albumin (0.964), total bilirubin (p = 0.086), and direct bilirubin (p = 0.779) were compared between cement occupationally exposed individuals and healthy non-exposed individuals at p < 0.05 (Table 2).

Table 2: Comparison of Hepatic Profiles of Cement Occupationally Exposed and Non-Exposed Individuals in Malete, Kwara State, Nigeria, 2022

Parameters	Cement-expose individuals	Non-exposed individuals	T-value	P-value
AST (U/L)	27.72±11.85	24.02±7.91	1.888	0.064
ALT (U/L)	30.58±11.54	19.90±7.26	5.758	0.000*
ALP (U/L)	181.68±26.25	163.68±29.92	3.279	0.002*
GGT (U/L)	21.95±6.49	21.65±7.76	0.205	0.838
Total Protein (g/L)	67.87±8.51	69.73±6.86	-1.260	0.213
Albumin (g/L)	39.85±3.97	39.88±3.67	-0.046	0.964
Total Bilirubin (µmol/L)	3.72±2.09	3.18±1.40	1.727	0.089
Direct Bilirubin (µmol/L)	1.18±0.82	1.22±0.81	-0.282	0.779

(*) means significant at $p < 0.05$.

Table 3 showed that the duration of cement dust exposure showed a positive correlation with AST ($r = 0.190$; $p = 0.147$), ALT ($r = 0.016$; $p = 0.904$), ALP ($r = 0.178$; $p = 0.175$), GGT ($r = 0.363$; $p = 0.004$) and direct bilirubin ($r = 0.057$; $p = 0.664$). Duration of Cement Dust Exposure showed a negative correlation with Total Protein ($r = -0.098$; $p = 0.455$), Albumin ($r = -0.097$; $p = 0.461$), and Total Bilirubin ($r = -0.156$; $p = 0.233$).

Table 3: Relationship between Duration of Cement Dust Exposure and Hepatic Profile in Cement Occupationally Exposed Individuals in Malete, Kwara State, Nigeria, 2022

Duration of Cement Dust Exposure		
Variables	Correlation	P-value
AST (U/L)	0.190	0.147
ALT (U/L)	0.016	0.904
ALP (U/L)	0.178	0.175
GGT (U/L)	0.363	0.004*
Total Protein (g/L)	-0.098	0.455
Albumin (g/L)	-0.097	0.461
Total Bilirubin (µmol/L)	-0.156	0.233
Direct Bilirubin (µmol/L)	0.057	0.664

(*) means significant at $p < 0.05$

Discussion

The cement industry is regarded as a major polluter due to the dust and particle matter released during the various stages of cement manufacture. Workers are typically exposed to dust via dermal and respiratory pathways, as well as, to a lesser extent, ingestion [20]. Cement dust inclusion particles, diffuse swelling, proliferation of hepatic sinusoi-

dal lining cells, sarcoid granulomas, and perisinusoidal and portal fibrosis have all been observed in the hepatocytes of cement mill workers [21]. These changes have been linked to hepatic lesions caused by inhaled cement dust [9].

In this study, we observed that ALT significantly increased at in cement occupationally exposed individuals compared to non-exposed individuals. This finding is consistent with the studies of Al Salhen *et al.* [22] and Richard *et al.* [1], who reported significant increases in ALT activities in cement handlers. ALT is of value as it indicates the existence of liver diseases, as this enzyme is present in large quantities in the liver. It increases in serum when cellular degeneration or destruction occurs in this organ [23]. Higher plasma ALT activities in cement handlers have also been reported by Malekirad *et al.* [24] and Owonikoko *et al.* [25]. However, this finding disagrees with the findings of Mojiminiyi *et al.* [26], who reported a decrease in ALT activity in cement handlers.

We also observed an insignificant increase in aspartate transaminase (AST) of cement occupationally exposed individuals compared to non-exposed individuals. This is consistent with previous studies by Festus *et al.* [12]. However, our findings disagree with Al Salhen *et al.* [22] and Richard *et al.* [1], who reported a significant increase in AST activities in cement handlers, and Mojiminiyi *et al.* [26], who reported a general decrease in AST activity in cement handlers. Also, Akhter *et al.* [27] reported non-significantly lower AST activities in the case group compared to the control group of cement factory workers.

Furthermore, our study demonstrated that alkaline phosphatase (ALP) significantly increased in cement occupationally

exposed individuals compared to non-exposed individuals. The increase in alkaline phosphatases in plasma caused by exposure to cement dust agrees with the findings of Orman *et al.* [28], Al Salhen *et al.* [22], and Richard *et al.* [1]. Conversely, our study disagrees with Festus *et al.* [12], who reported no significant change in ALP, and Mojiminiyi *et al.* [26], who reported a decrease in ALP activity in cement handlers. Alkaline phosphatases comprise a group of enzymes that catalyze the hydrolysis of phosphate esters in an alkaline environment, generating an organic radical and inorganic phosphate [29]. In healthy adults, this enzyme is mainly derived from the liver, and its increased serum level is seen in liver disease associated with extra or intra-hepatic obstruction, obstructive jaundice, infectious mononucleosis, biliary cirrhosis, and cholestasis [30] [31].

In addition, there was no significant change observed in GGT between cement occupationally exposed individuals compared to non-exposed individuals. This is in contrast to the study of Zawilla *et al.* [32], who reported a significant increase in GGT in occupationally exposed individuals. The reason for variation in the studies could be due to the duration of exposure to cement dust on Gamma Glutamyl Transferase, which showed a significant positive correlation in the present study. This suggests that long-term or chronic exposure to cement dust could have deleterious effects on Gamma Glutamyl Transferase.

Total protein and albumin were observed to be insignificantly decreased in cement occupationally exposed individuals compared to non-exposed individuals at which agrees with Sameen [33] and Ogunbileje and Akinosun [34], who reported no significant difference in total protein and albumin levels in cement-exposed workers in Al-Ramadi city, Iraq, and Nigeria, respectively. However, our findings are in discordance with Oluwayemisi [35], who reported a significant decrease in total protein and albumin.

Moreso, no significant difference was observed in total and direct bilirubin of cement occupationally exposed individuals and non-exposed individuals. This agrees with the study of Ashwini *et al.* [36], Idris *et al.* [37], and Ogeniyi *et al.* [38], who reported no significant difference in total and conjugated bilirubin in cement handlers compared with non-cement handlers and with an insignificant perturbation in liver function. This observation is in discordance with the findings of Richard *et al.* [1], who reported an increase in the level of total

and conjugated bilirubin in cement handlers. Similarly, Krishna *et al.* [39] reported a significant increase in plasma bilirubin levels of cement handlers; however, Mojiminiyi *et al.* [26] reported a general decrease in plasma total and conjugated bilirubin levels of cement factory workers compared with those of the control subjects.

The findings of this study have shown that occupational exposure to cement dust can be a potential for future development of hepatotoxicity, as ALT and ALP levels were significantly increased. Due to the high concentration of ALT in the liver, it is useful in detecting the presence of liver disease. It rises in serum levels when this organ experiences cellular degeneration or injury [40–50]. Increased Alanine aminotransaminases and alkaline phosphatase activities indicate toxicity and liver injury.

Conclusion

Cement-exposed individuals exhibited elevated levels of liver enzymes such as Alanine transaminase and alkaline phosphatase, suggesting potential liver impairment. Liver dysfunction typically manifests when 60% of hepatocytes are affected. This increase in enzyme levels may indicate potential hepatotoxic complications.

Recommendation

The observations from our study emphasize the need for adequate safety and precautionary measures among cement-exposed individuals.

Limitations

A limitation of this study is the relatively small sample size, which may limit the generalizability of the findings. Further research with a larger sample size is warranted to confirm these results.

Acknowledgment

The authors express gratitude to God for the grace they received to complete this work and to individuals who consented to participate in the study.

Funding

This research was funded by the authors.

Conflict of interest

The authors of this work declare no conflict of interest.

Reference

1. Richard EE, Augusta Chinyere NA, Jeremaiah OS, Opara UC, Henrieta EM, Ifunanya ED. Cement Dust Exposure and Perturbations in Some Elements and Lung and Liver Functions of Cement Factory Workers. *J Toxicol.* 2016;2016:6104719. doi:10.1155/2016/6104719
2. Schenker MB, Pinkerton KE, Mitchell D, Vallyathan V, Elvine-Kreis B, Green FH. Pneumoconiosis from agricultural dust exposure among young California farm workers. *Environ Health Perspect.* 2009;117(6):988-994. doi:10.1289/ehp.0800144
3. Gbadebo AM, Bankole OD. Analysis of potentially toxic metals in airborne cement dust around Sagamu, Southwestern Nigeria. *Journal of Applied Sciences.* 2007 Jan;7(1):35-40.
4. Hoy R, Yates DH. Artificial stone-associated silicosis in Belgium: response. *Occup Environ Med.* 2019;76(2):134. doi:10.1136/oemed-2018-105563
5. Abdelhamid A. Effect of Exposure to Portland Cement Dust on the Periodontal Status and on the Outcome of Non-Surgical Periodontal Therapy. *Int J Health Sci (Qassim).* 2016;10(3):339-352.
6. Aydin S, Croteau G, Sahin I, Citil C. Ghrelin, nitrite, and paraoxonase/arylesterase concentrations in cement plant workers. *Journal of Medical Biochemistry.* 2010 Apr 1;29(2):78.
7. Al-Otaibi FS, Ajarem JS, Abdel-Maksoud MA, et al. Stone quarrying induces organ dysfunction and oxidative stress in *Meriones libycus*. *Toxicol Ind Health.* 2018;34(10):679-692. doi:10.1177/0748233718781290
8. Choudhry RM. Behavior-based safety on construction sites: a case study. *Accid Anal Prev.* 2014;70:14-23. doi:10.1016/j.aap.2014.03.007
9. Ngombe LK, Nlandu RN, Ngombe DK, Ilunga BK, Okitotsho SW, Sakatolo JB, Numbi OL, Danuser B. Respiratory health of dust-exposed cement carriers in Haut-Katanga province, DR Congo. *Environnement, Risques & Santé.* 2019 Nov 1;18(6):500-7.
10. Sawyerr H, Salako G, Olalubi O, Adio A, Adebayo A, Badmos B, Jambo UM, Adepoju G. Spatio Temporal Land Use Land Cover Change Mapping of Maleta Elemere: Implication on Development Planning of Emerging Communities. *International Journal of Environment, Agriculture and Biotechnology.*;2(4):238879.
11. Wang, H., & Chow, S.-C. (2007). *Sample Size Calculation for Comparing Proportions.* *Wiley Encyclopedia of Clinical Trials.* doi:10.1002/9780471462422.eoc
12. Festus OO, Agbebaku SO, Idonije BO, Oluba OM. Influence of Cement Dust Exposure on Indicators of Hepatic Function in Male Cement Handlers in Ekpoma, Nigeria. *Electronic Journal of Medical and Educational Technologies.* 2021 Apr 1;14(2):em2104.
13. Doumas BT, Watson WA, Biggs HG. Albumin standards and the measurement of serum albumin with bromocresol green. *Clin Chim Acta.* 1971;31(1):87-96. doi:10.1016/0009-8981(71)90365-2
14. Tietz NW. Clinical guide to laboratory tests. In *Clinical guide to laboratory tests 1995* (pp. 1096-1096).
15. Lorentz K. Approved recommendation on IFCC methods for the measurement of catalytic concentration of enzymes. Part 9. IFCC method for alpha-amylase (1,4-alpha-D-glucan 4-glucanohydrolase, EC 3.2.1.1). International Federation of Clinical Chemistry and Laboratory Medicine (IFCC). Committee on Enzymes. *Clin Chem Lab Med.* 1998;36(3):185-203. doi:10.1515/CCLM.1998.034
16. REITMAN S, FRANKEL S. A colorimetric method for the determination of serum glutamic oxalacetic and glutamic pyruvic transaminases. *Am J Clin Pathol.* 1957;28(1):56-63. doi:10.1093/ajcp/28.1.56
17. King EJ, Armstrong AR. A CONVENIENT METHOD FOR DETERMINING SERUM AND BILE PHOSPHATASE ACTIVITY. *Can Med Assoc J.* 1934;31(4):376-381.
18. Jendrassik L, Grof P. Colorimetric method for estimation of serum bilirubin. *Biochemische Zeitschrift.* 1938;2(297):81.
19. Szasz G. Reaction-rate method for gamma-glutamyltransferase activity in serum. *Clin Chem.* 1976;22(12):2051-2055.
20. Alshammari FD, Hommi BS, Ahmed HG. Assessment of Infectious and Inflammatory changes in sputum associated with cement dust. *Egyptian Academic Journal of Biological Sciences, G. Microbiology.* 2014 Dec 1;6(2):33-40.
21. Sah DP, Chaudhary S, Shakya R, Mishra AK. Occupa-

- tional accidents in cement industries of Nepal. *J Adv Res Altern Energy, Environ Ecol.* 2019;6(3&4):22-8.
22. Al Salhen KS. Assessment of oxidative stress, haematological, kidney and liver function parameters of Libyan cement factory workers. *Journal of American Science.* 2014;10(5):58-65.
 23. Elagib MF, Ghandour IA, Abdel Rahman ME, Baldo SM, Idris AM. Influence of cement dust exposure on periodontal health of occupational workers. *Toxin Reviews.* 2021 Oct 2;40(4):1496-504.
 24. Malekirad AA, Rahzani K, Ahmadi M, Rezaei M, Abdollahi M, Shahrjerdi S, Roostaie A, Mohajerani HR, Boland Nazar NS, Torfi F, Mousavi Khaneghah A. Evaluation of oxidative stress, blood parameters, and neurocognitive status in cement factory workers. *Toxin Reviews.* 2021 Oct 2;40(4):1128-34.
 25. Mojiminiyi FB, Merenu IA, Ibrahim MT, Njoku CH. The effect of cement dust exposure on haematological and liver function parameters of cement factory workers in Sokoto, Nigeria. *Niger J Physiol Sci.* 2008;23(1-2):111-114. doi:10.4314/njps.v23i1-2.54945
 26. Owonikoko MW, Salami AT, Odukanmi AO, Emikpe BO, Olaleye SB. Cement dust inhalation induces hepatorenal dysfunction via tissue heavy metal bioaccumulation, histopathological and biochemical mechanisms. *Comparative Clinical Pathology.* 2023 Dec;32(6):1019-33.
 27. Akhter S, Khan MS, Akhter M, Datta A, Begum M. Effects of Cement Dust on Liver Function Parameters of Some Cement Factory Workers. *Chattagram Maa-O-Shishu Hospital Medical College Journal.* 2022 Dec 8;21(2):22-4.
 28. Orman A, Kahraman A, Cakar H, Ellidokuz H, Serteser M. Plasma malondialdehyde and erythrocyte glutathione levels in workers with cement dust-exposure [corrected] [published correction appears in *Toxicology.* 2005 Nov 5;215(1-2):170]. *Toxicology.* 2005;207(1):15-20. doi:10.1016/j.tox.2004.07.021
 29. Mohammadi S, Mehrparvar A, Labbafinejad Y, Attarchi MS. The effect of exposure to a mixture of organic solvents on liver enzymes in an auto manufacturing plant. *Journal of Public Health.* 2010 Dec;18:553-7.
 30. Kechrid Z, Kenouz R. Determination of alkaline phosphatase activity in patients with different zinc metabolic disorders. *Turkish Journal of Medical Sciences.* 2003;33(6):387-91.
 31. Khanna S, Kumar A. Infectious mononucleosis presenting as acute hepatitis, with marked leukocytosis and renal involvement. *Indian J Gastroenterol.* 2003;22(2):62.
 32. Zawilla N, Taha F, Ibrahim Y. Liver functions in silica-exposed workers in Egypt: possible role of matrix remodeling and immunological factors. *Int J Occup Environ Health.* 2014;20(2):146-156. doi:10.1179/2049396714Y.0000000061
 33. Sameen AM. Study the effect of cement dust exposure on liver and kidney parameters in some cement field workers in Al-Ramadi City. *J. of the University of Anbar for pure science.* 2013;7(2).
 34. Ogunbileje JO, Akinosun OM. Biochemical and haematological profile in Nigerian cement factory workers. *Research Journal of Environmental Toxicology.* 2011;5(2):133-40.
 35. Bamidele TO, Atolaye BO. Antioxidant Status And Hepatic Lipid Peroxidation In Albino Rats Exposed To Cement Dust. *Transnational Journal Of Science And Technology.* 2012 May:50.
 36. Ashwini S, Swathi K, Saheb SH. Effects of cement dust on hematological and liver function test parameters. *International Journal of Current Pharmaceutical & Clinical Research.* 2016;6(2):70-3.
 37. Idris SB, Musbahu L, Mayaki AM. Effect of cement kiln dust exposure on haematological and liver function parameters of sheep raised around Sokoto cement factory. *MOJ Toxicology.* 2018;4:340-3.
 38. Krishna L, Sampson U, Annamala PT, et al. Genomic Instability in Exfoliated Buccal Cells among Cement Warehouse Workers. *Int J Occup Environ Med.* 2020;11(1):33-40. doi:10.15171/ijoem.2020.1744
 39. Ogenyi SI, Ike AO, Blessing OC, Eberechukwu GS, Chinemerem A, Hanson SI. Exposure-time effect of cement dust on liver organ in rat (*Rattus norvegicus*). *Biotechnology Journal International.* 2022 Dec 29;26(6):32-40.
 40. Idonije BO, Nwoke EO, Festus O, Oluba OM. Plasma concentrations of kidney function indicators in malaria patients in Ekpoma, South-South Nigeria. *International Journal of Tropical Medicine.* 2011;6(1):4-7.
 41. Onyeneke EC, Oluba OM, Ojeaburu SI, Adeyemi O, Eriyamremu GE, Adebisi KE. Effect of soy protein on serum lipid profile and some lipid-metabolizing enzymes

- in cholesterol fed rats. *African Journal of Biotechnology*. 2007;6(19):2267-2273.
42. Owonikoko MW, Emikpe BO, Olaleye SB. Standardized experimental model for cement dust exposure; tissue heavy metal bioaccumulation and pulmonary pathological changes in rats. *Toxicology reports*. 2021 Jan 1;8:1169-78.
43. Tajudeen Y, Okpuzor J, Fausat AT. Investigation of general effects of cement dust to clear the controversy surrounding its toxicity. *Asian J Sci Res*. 2011;4(4):315-25.
44. Aminian O, Aslani M, Haghighi KS. Cross-shift study of acute respiratory effects in cement production workers. *Acta Medica Iranica*. 2014:146-52.
45. Jaishankar M, Tseten T, Anbalagan N, Mathew BB, Beeregowda KN. Toxicity, mechanism and health effects of some heavy metals. *Interdiscip Toxicol*. 2014;7(2):60-72. doi:10.2478/intox-2014-0009
46. Brzóska MM, Moniuszko-Jakoniuk J, Piłat-Marcinkiewicz B, Sawicki B. Liver and kidney function and histology in rats exposed to cadmium and ethanol. *Alcohol Alcohol*. 2003;38(1):2-10. doi:10.1093/alcalc/agg006
47. Ezedom T, Asagba S, Tonukari NJ. Toxicological effects of the concurrent administration of cadmium and arsenic through the food chain on the liver and kidney of rats. *The Journal of Basic and Applied Zoology*. 2020 Dec;81:1-2.
48. Hermenean A, Damache G, Albu P, et al. Histopathological alterations and oxidative stress in liver and kidney of *Leuciscus cephalus* following exposure to heavy metals in the Tur River, North Western Romania. *Ecotoxicol Environ Saf*. 2015;119:198-205. doi:10.1016/j.ecoenv.2015.05.029
49. Laniyan TA, Adewumi AJ. Evaluation of contamination and ecological risk of heavy metals associated with cement production in Ewekoro, Southwest Nigeria. *Journal of Health and Pollution*. 2020 Mar 1;10(25):200306.
50. Sagi Tanju ST, Madhuri D. Arsenic induced oxidative stress, hemato-biochemical and histological changes in liver and protective effect of Moringa leaf powder and ascorbic acid in broiler chicken. *J Chem Pharma Res*, 2013, 5(2):112–16.